

Scalable, self-verifying variational quantum eigensolver using adiabatic warm starts

Bojan Žunkovič^{1, 2, *} Marco Ballarin³, Lewis Wright³ and Michael Lubasch^{3, †}

¹ University of Ljubljana, Faculty of Computer and Information Science, Večna pot 113, 1000 Ljubljana, Slovenia

² Rudolfovo, Science and Technology Centre, Novo mesto, Slovenia

³ Quantinuum, Partnership House, Carlisle Place, London SW1P 1BX, United Kingdom

(Dated: February 19, 2026)

We study an adiabatic variant of the variational quantum eigensolver (VQE) in which VQE is performed iteratively for a sequence of Hamiltonians along an adiabatic path. We derive the conditions under which gradient-based optimization successfully prepares the adiabatic ground states. These conditions show that the barren plateau problem and local optima can be avoided. Additionally, we propose using energy-standard-deviation measurements at runtime to certify eigenstate accuracy and verify convergence to the global optimum.

Introduction — The variational quantum eigensolver (VQE) is a promising algorithm for ground-state preparation on current noisy intermediate-scale quantum (NISQ) computers [1–3]. In its traditional formulation, however, VQE faces significant obstacles, such as challenging optimization landscapes characterized by barren plateaus [4] and numerous local optima [5], as well as the absence of an intrinsic mechanism for the verification of the correctness of the obtained solutions [6].

An alternative to VQE, that can avoid these obstacles, is adiabatic ground-state preparation. In its standard circuit-model implementation [7, 8], however, this approach often generates quantum circuits that are too deep to be feasible on NISQ devices. Although various NISQ-compatible schemes have been proposed [9–26] — most of which combine adiabatic concepts with variational quantum algorithms — they lack rigorous convergence guarantees.

Closely related to adiabatic methods is the concept of a warm start that has recently gained attention in variational quantum optimization [27–29]. The central idea is to optimize the variational ansatz incrementally along a predefined optimization path. At each point on this path, the optimizer initializes the ansatz with the parameters obtained at the previous point, thereby warm-starting the optimization. It has been shown that warm-start strategies can provably avoid the barren plateau problem in variational quantum simulation [27] and multivariate state preparation [29].

In this paper, we analyze the warm-start paradigm in an adiabatic VQE (AVQE) where VQE is executed sequentially along the Hamiltonians of a discretized adiabatic path. We determine the conditions under which *gradient descent tracks the instantaneous ground states*, introduce a *runtime verification* procedure based on the energy standard deviation, provide gap-conditional correctness certificates, and demonstrate robustness against measurement shot noise. Figure 1 visualizes our key findings. Our results establish that, by leveraging adiabaticity, VQE overcomes its main obstacles and can be formulated as a scalable, self-verifying algorithm for ground-state

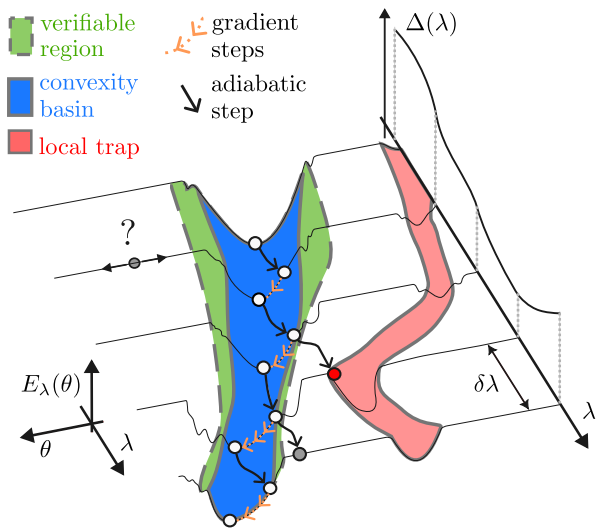


FIG. 1. AVQE optimization landscape — Consider a Hamiltonian $H(\lambda)$ where $\lambda \in [0, 1]$ defines an adiabatic path, a variational ansatz parameterized by θ , and the associated energy-based cost function $E_\lambda(\theta)$. Starting from the ground state at $\lambda = 0$, there exists a basin (blue) that follows the adiabatic path and guarantees convexity. The size of the convexity basin decreases at most linearly with the instantaneous gap $\Delta(\lambda)$ (black curve, right-hand 2D plot) which denotes the energy difference between the ground and first excited state at λ . Outside the convexity basin, the optimization landscape may exhibit barren plateaus (white) and local minima (red), which can hinder gradient-based optimization. In the verifiable region (green), which also scales linearly with $\Delta(\lambda)$, we cannot assume convexity, but we can check that the closest eigenstate is the ground state. This enables adaptation of the adiabatic step width $\delta\lambda$ to ensure provable convergence to the target ground state at $\lambda = 1$.

computations using NISQ hardware.

Setup — We consider a linear adiabatic schedule defined by the Hamiltonian

$$H(\lambda) = (1 - \lambda)H_i + \lambda H_f, \quad \lambda \in [0, 1], \quad (1)$$

where the initial Hamiltonian H_i is chosen to have an easy-to-prepare ground state and the final Hamiltonian

H_f encodes the desired target ground state. We denote the instantaneous ground state by $|\psi_0(\lambda)\rangle$, the spectral gap by

$$\Delta(\lambda) = E_1(\lambda) - E_0(\lambda) \quad (2)$$

where $E_0(\lambda)$ is the ground and $E_1(\lambda)$ the first-excited-state energy at λ , and we denote the minimum gap along the path by

$$\Delta_{\min} = \min_{\lambda \in [0,1]} \Delta(\lambda). \quad (3)$$

We use the variational ansatz

$$|\psi(\boldsymbol{\theta})\rangle = \prod_{j=0}^{M-1} U_j |0\rangle, \quad U_j = e^{-iP_j \theta_j}, \quad (4)$$

where bold symbols denote vectors and $P_j \in \{I, X, Y, Z\}^{\otimes n}$. The theorems presented in the paper can also be derived without any reference to the specific variational ansatz. In that case, however, we cannot obtain the explicit dependence of the number of gradient steps on the number of variational parameters.

The variational energy at fixed λ is

$$E_\lambda(\boldsymbol{\theta}) = \langle \psi(\boldsymbol{\theta}) | H(\lambda) | \psi(\boldsymbol{\theta}) \rangle, \quad (5)$$

and we denote by $\boldsymbol{\theta}^*(\lambda)$ a global minimizer satisfying $|\psi(\boldsymbol{\theta}^*(\lambda))\rangle = |\psi_0(\lambda)\rangle$.

The variational manifold is equipped with the real metric

$$g_{\mu\nu}(\boldsymbol{\theta}(\lambda)) = \text{Re}(\langle \partial_\mu \psi | \partial_\nu \psi \rangle - \langle \partial_\mu \psi | \psi \rangle \langle \psi | \partial_\nu \psi \rangle), \quad (6)$$

which determines the local behaviour of the variational optimization landscape.

We discretize the adiabatic parameter into T slices,

$$\lambda_t = t \delta\lambda, \quad \delta\lambda = \frac{1}{T}, \quad t = 0, 1, \dots, T, \quad (7)$$

and perform optimization sequentially along the path using warm starts. We initialize $\boldsymbol{\theta}_0$ such that $|\psi(\boldsymbol{\theta}_0)\rangle = |\psi_0(0)\rangle$. For each slice $t = 1, \dots, T$, we run K steps of gradient-based optimization on E_{λ_t} , starting from the previous parameter values $\boldsymbol{\theta}_{t-1}$:

$$\boldsymbol{\theta}_t^{(0)} = \boldsymbol{\theta}_{t-1}^{(K)}, \quad (8)$$

$$\boldsymbol{\theta}_t^{(k+1)} = \boldsymbol{\theta}_t^{(k)} - \eta \mathcal{G}_t(\boldsymbol{\theta}_t^{(k)}), \quad k = 0, 1, \dots, K-1, \quad (9)$$

$$|\psi_t\rangle = \left| \psi(\boldsymbol{\theta}_t^{(K)}) \right\rangle, \quad (10)$$

where $\eta > 0$ is the learning rate and $-\mathcal{G}_t(\boldsymbol{\theta})$ denotes the chosen descent direction for the objective at $\lambda = \lambda_t$. In the simplest case, $\mathcal{G}_t(\boldsymbol{\theta}) = \nabla_{\boldsymbol{\theta}} E_{\lambda_t}(\boldsymbol{\theta})$ (vanilla gradient descent), but the protocol also covers natural-gradient or more advanced optimizers with momentum, such as [30, 31]. Overall, the procedure performs T parameter shifts

in λ and K optimization steps per shift, leading to a total of $N_{\text{updates}} = TK$ optimization updates.

For any operator A , $\|A\|_{\text{op}}$ represents its operator norm. If A depends on λ , we define $\|A\|_{\text{op}} = \max_{\lambda} \|A(\lambda)\|_{\text{op}}$. Its standard deviation with respect to $|\psi_t\rangle$ is defined as

$$\sigma_{\psi_t}(A) = \sqrt{\langle \psi_t | A^2 | \psi_t \rangle - (\langle \psi_t | A | \psi_t \rangle)^2}. \quad (11)$$

Throughout the paper, we use the following assumptions.

ASSUMPTION 1 (SPECTRAL GAP) The instantaneous ground state of $H(\lambda)$ is nondegenerate and $\Delta_{\min} > 0$.

ASSUMPTION 2 (EXACT REPRESENTABILITY) For all $\lambda \in [0, 1]$, there exists a parameter vector $\boldsymbol{\theta}^*(\lambda)$ such that

$$|\psi(\boldsymbol{\theta}^*(\lambda))\rangle = |\psi_0(\lambda)\rangle. \quad (12)$$

ASSUMPTION 3 (NONDEGENERATE GEOMETRY) There exists a constant $\gamma > 0$ such that, for all $\lambda \in [0, 1]$ and all $\boldsymbol{\theta}^*(\lambda)$, the geometric tensor obeys

$$\mathbf{g}(\boldsymbol{\theta}^*(\lambda)) \succeq \gamma \mathbb{I}. \quad (13)$$

Using these conditions, we prove two theorems that enable gap-conditioned, verifiable, variational ground-state tracking.

Adiabatic tracking via gradient descent — Let us first give a brief, informal summary of the central result of our adiabatic optimization approach: Gradient descent, as outlined in the preceding section, tracks the instantaneous ground state along the adiabatic path with N_{updates} that depends polynomially on the gap Δ_{\min} and the number of variational parameters M , and depends on the system size only through operator norms.

Theorem 1 (Adiabatic tracking) *Assume that Assumptions 1–3 hold and that the optimization protocol described above is used with the Pauli-rotation ansatz of Eq. 4 containing M parameters. Then there exist universal numerical constants $c_0, c_1 > 0$ such that the following holds.*

If the adiabatic discretization satisfies

$$\delta\lambda \leq \delta\lambda_A = c_0 \frac{\gamma^2 \Delta_{\min}^2}{M^2 \|H\|_{\text{op}} \|\partial_\lambda H\|_{\text{op}}} \quad (14)$$

and the number of optimization steps per slice satisfies

$$K \geq c_1 \frac{M \|H\|_{\text{op}}}{\gamma \Delta_{\min}}, \quad (15)$$

then the optimised parameters $\boldsymbol{\theta}_t^{(k)}$ track, for $k = 0, \dots, K$, the instantaneous ground state along the entire path in the sense that

$$\|\boldsymbol{\theta}_t^{(k)} - \boldsymbol{\theta}^*(\lambda_t)\|_2 \leq \frac{\gamma \Delta_{\min}}{48 M^{3/2} \|H\|_{\text{op}}}, \quad t = 0, 1, \dots, T. \quad (16)$$

In [32] we show that the condition of Eq. 16 guarantees that the optimisation at any step converges to the actual ground state $|\psi_0(\lambda_t)\rangle$ and requires only a logarithmic overhead if a specific fidelity is targeted.

We present two complementary proofs of Theorem 1 in [32]. The first is based on the Polyak–Lojasiewicz condition [33], while the second relies on the time-dependent variational principle for imaginary time [34]. The former describes the optimization geometry induced by the spectral gap and establishes strong convexity, ensuring contraction of the energy error and convergence of the parameters. The latter interprets the algorithm as a discretized imaginary-time evolution and clarifies how the spectral gap controls the stability of adiabatic tracking. While leading to the same convergence guarantees, the two derivations isolate distinct mechanisms underlying variational tracking — optimization curvature versus dynamical stability.

The total number of optimization updates obeys the explicit scaling

$$N_{\text{updates}} = \mathcal{O}\left(\frac{\|H\|_{\text{op}}^2 M^3 \|\partial_\lambda H\|_{\text{op}}}{\gamma^3 \Delta_{\min}^3}\right). \quad (17)$$

Notably, the scaling with the gap is worse than the expected $\mathcal{O}(1/\Delta_{\min}^2)$ scaling observed in the adiabatic theorem [35]. As we show in [32], the additional $1/\Delta_{\min}$ factor arises from the stability of the numerical integration scheme and cannot be avoided using more sophisticated (e.g., implicit) integrators. Physically, the observed $\mathcal{O}(\Delta_{\min}^{-3})$ scaling admits an intuitive interpretation: Adiabatic passage slows down as $T \propto \Delta_{\min}^{-2}$, while variational tracking requires repeated relaxation towards the instantaneous ground state whose cooling time is determined by the gap and scales as $\mathcal{O}(\Delta_{\min}^{-1})$.

Compared to standard quantum annealing [36, 37], the Theorem 1 has larger gap complexity. However, AVQE can offer greater control over the schedule and additional options for hybrid quantum-classical optimization, which are not possible in real-time analog quantum annealing. In particular, the gap does not determine the coherence time of the variational ansatz but rather the number of optimization steps, which can be beneficial in noisy devices, assuming the required circuit depth is not too big. Moreover, we can adjust the step size $\delta\lambda$ based on an approximation of the gap. Also, we can offload the initial, easy part of the annealing evolution to a classical device and use the quantum device only if the classical variational ansatz is not expressive enough.

As a side result, because the optimization stays in a locally well-conditioned region, gradients remain nonvanishing along the adiabatic path. Avoidance of barren plateaus follows directly from adiabatic tracking and is not imposed as an independent assumption. We additionally prove in [32] that gradient magnitudes are guaranteed to be sufficiently large around the adiabatic variational

minimum in a region scaling as $\mathcal{O}\left(\gamma\Delta_{\min}/(M^{3/2}\|H\|_{\text{op}})\right)$.

Runtime verification via standard deviation — Theorem 1 establishes sufficient conditions for tracking the instantaneous ground state along the adiabatic path. However, it does not provide an *a posteriori* certification procedure: It offers no mechanism to assess whether the variational state obtained at a given step is close to an exact eigenstate, nor to verify that the final state coincides with the target ground state.

In this section, we introduce a runtime verification criterion based on the energy standard deviation, inspired by [38]. This criterion guarantees that the variational state is associated with a unique eigenstate branch and, given a lower bound on the spectral gap, certifies that this branch corresponds to the ground state.

Theorem 2 (Runtime verification) *Assume that there exists a constant $\Delta_c > 0$ such that $\Delta_c \leq \Delta_{\min}$. If, for all $t = 0, 1, \dots, T$,*

$$\sigma_{\psi_t}(H(\lambda_t)) < \frac{\Delta_c}{2} \quad (18)$$

and the adiabatic step size satisfies

$$\delta\lambda < \delta\lambda_V = \frac{\Delta_c - \sigma_{\psi_t}(H(\lambda_t))}{2\sigma_{\psi_t}(H_f - H_i)}, \quad (19)$$

then the state $|\psi_t\rangle$ is uniquely associated with the ground-state eigenbranch of $H(\lambda_t)$ and obeys the fidelity bound

$$|\langle\psi_0(\lambda_t)|\psi_t\rangle|^2 \geq \frac{8}{9}. \quad (20)$$

The theorem tells us that, if a gap lower bound $\Delta_c \leq \Delta_{\min}$ is available, then the standard deviation condition $\sigma_{\psi_t}(H(\lambda_t)) < \Delta_c/2$ provides a sufficient, runtime-verifiable certificate that the variational state approximates the actual ground state with fidelity exceeding 8/9. The proof of Theorem 2 is presented in [32].

We note that for both theorems, Assumption 2 can be relaxed to allow for approximate representability where the variational manifold contains the exact ground state up to the energy error $\epsilon < \frac{\Delta_c}{4}$ [32]. In this case, tracking remains in place with the replacement $\Delta_{\min} \rightarrow \Delta_{\min} - \epsilon$, and the verification theorem remains unchanged [32].

Algorithm — The tracking and verification components combine naturally into an adiabatic variational quantum optimization protocol. Algorithm 1 explicitly implements the guarantees of Theorem 1 and 2: The optimization steps enforce adiabatic tracking, and the energy standard deviation measurements provide runtime verification (i.e., we are tracking an eigenstate with a lower bound on the fidelity) and gap-conditional certification (i.e., if the standard deviation is sufficiently smaller than the gap, then the tracked state is the ground state).

Algorithm: Self-verifying AVQE

Input: Initial Hamiltonian H_i , final Hamiltonian H_f , initial parameters θ_0 , adiabatic tracking step size $\delta\lambda_A$, learning rate η , number of gradient steps K , estimated gap bound Δ_c

Output: Final variational state $|\psi(\theta)\rangle$

- 1: Prepare $|\psi(\theta_0)\rangle$ as the ground state of $H(0)$
- 2: $\lambda \leftarrow 0$
- 3: **while** $\lambda < 1$ **do**
- 4: Perform K gradient-descent steps on $E_\lambda(\theta)$
- 5: Measure $\sigma_\psi(H(\lambda))$
- 6: **if** $\sigma_\psi(H(\lambda)) > \Delta_c/2$ **then**
- 7: **go to line 4**
- 8: **end if**
- 9: Measure $\sigma_\psi(H_f - H_i)$
- 10: $\delta\lambda_V \leftarrow \frac{\Delta_c/2 - \sigma_\psi(H(\lambda))}{\sigma_\psi(H_f - H_i)}$
- 11: $\delta\lambda \leftarrow \min\{\delta\lambda_A, \delta\lambda_V, 1 - \lambda\}$
- 12: $\lambda \leftarrow \lambda + \delta\lambda$
- 13: **end while**
- 14: **return** $|\psi(\theta)\rangle$

The algorithmic parameters K , $\delta\lambda_A$, and η may be chosen according to Theorem 1 or treated as hyperparameters and selected via empirical optimization.

The algorithm assumes knowledge of a lower bound of the gap. In the absence of such a lower bound, one possibility is to estimate Δ_c and run the protocol starting from that estimate, successively reducing it until the energy converges.

Shot-noise robustness — In realistic implementations, gradients and observables are estimated from a finite number of measurement shots. Under standard shot-noise models [32], the resulting stochastic gradients remain unbiased and concentration bounds imply that, with high probability, the optimization dynamics stay within the tracking region identified in Theorem 1. In this regime, shot noise modifies convergence rates but does not destabilize adiabatic tracking.

The standard-deviation-based verification remains valid in the presence of shot noise, provided the measurement budget is chosen such that statistical fluctuations in the estimated standard deviations are smaller than the spectral gap threshold. In particular, a number of shots per slice scaling as $\mathcal{O}(\Delta_{\min}^{-4})$ suffices to preserve the certification guarantees with high probability. Consequently, statistical noise affects only the quantitative efficiency of the protocol and does not alter its logical structure: tracking, verification, and gap-conditional certification remain intact.

Discussion — Our results establish a principled paradigm for variational quantum algorithms. The resulting algorithm is among the few NISQ-compatible quantum algorithms that admit *provable correctness guarantees*. Under explicit and verifiable conditions, the protocol certifies both successful tracking of the target eigenstate and, conditioned on a gap bound, preparation of the actual ground state. This distinguishes the approach from most

existing variational algorithms, which rely on heuristic convergence diagnostics and lack rigorous success criteria.

From an optimization perspective, the framework directly tackles two central challenges in variational quantum optimization. Firstly, adiabatic warm-starting combined with local tracking circumvents barren plateaus and enables efficient optimization by restricting optimization to a continuously connected, well-behaved region. Secondly, the combination of path-following and standard-deviation-based verification suppresses convergence to spurious local minima by enforcing consistency with an underlying physical ground-state branch throughout the evolution.

More broadly, the framework provides a rigorous foundation for developing new classes of hybrid quantum-classical algorithms. An interesting next step is to reformulate the tools developed here for adiabatic time evolution, enabling us to track eigenstates other than the ground state. In this context, there are numerous important applications, ranging from excited-state computations to the solution of linear systems of equations [39–41]. Another interesting next step is to explore how experimental noise and gate errors affect our algorithm and whether we can develop noise-mitigation techniques tailored to our approach. By replacing heuristic stopping rules with principled runtime verification and gap-conditional certification, our approach opens a systematic route toward reliable variational algorithms in the NISQ and early fault-tolerant era.

Note — Recently, a related article appeared on the arXiv [42], in which the authors show that, by making use of adiabaticity, VQE optimization can avoid the barren plateau problem. Here, we additionally show that AVQE can prepare ground states with rigorous accuracy guarantees by using energy-standard-deviation measurements.

Acknowledgement — BZ was funded by the ARIS project J2-60034, the ARIS research program P2-0209 Artificial Intelligence and Intelligent Systems (2022 – 2024), and the UL-VIP project under contract no. SN-ZRD/22-27/0510.

* bojan.zunkovic@fri.uni-lj.si
 † michael.lubasch@quantinuum.com

[1] M. Cerezo, A. Arrasmith, R. Babbush, S. C. Benjamin, S. Endo, K. Fujii, J. R. McClean, K. Mitarai, X. Yuan, L. Cincio, and P. J. Coles, Variational quantum algorithms, *Nat. Rev. Phys.* **3**, 625 (2021).

[2] K. Bharti, A. Cervera-Lierta, T. H. Kyaw, T. Haug, S. Alperin-Lea, A. Anand, M. Degroote, H. Heimonen, J. S. Kottmann, T. Menke, W.-K. Mok, S. Sim, L.-C. Kwek, and A. Aspuru-Guzik, Noisy intermediate-scale quantum algorithms, *Rev. Mod. Phys.* **94**, 015004 (2022).

[3] J. Tilly, H. Chen, S. Cao, D. Picozzi, K. Setia, Y. Li, E. Grant, L. Wossnig, I. Rungger, G. H. Booth, and

J. Tennyson, The Variational Quantum Eigensolver: A review of methods and best practices, *Phys. Rep.* **986**, 1 (2022).

[4] M. Larocca, S. Thanasilp, S. Wang, K. Sharma, J. Biamonte, P. J. Coles, L. Cincio, J. R. McClean, Z. Holmes, and M. Cerezo, Barren plateaus in variational quantum computing, *Nat. Rev. Phys.* **7**, 174 (2025).

[5] E. R. Anschuetz and B. T. Kiani, Quantum variational algorithms are swamped with traps, *Nat. Commun.* **13**, 7760 (2022).

[6] A. Gheorghiu, T. Kapourniotis, and E. Kashefi, Verification of Quantum Computation: An Overview of Existing Approaches, *Theory Comput. Syst.* **63**, 715 (2019).

[7] E. Farhi, J. Goldstone, S. Gutmann, and M. Sipser, Quantum Computation by Adiabatic Evolution (2000), [arXiv:quant-ph/0001106 \[quant-ph\]](https://arxiv.org/abs/quant-ph/0001106).

[8] T. Albash and D. A. Lidar, Adiabatic quantum computation, *Rev. Mod. Phys.* **90**, 015002 (2018).

[9] E. Farhi, J. Goldstone, and S. Gutmann, A Quantum Approximate Optimization Algorithm (2014), [arXiv:1411.4028 \[quant-ph\]](https://arxiv.org/abs/1411.4028).

[10] D. Wecker, M. B. Hastings, and M. Troyer, Progress towards practical quantum variational algorithms, *Phys. Rev. A* **92**, 042303 (2015).

[11] A. Garcia-Saez and J. I. Latorre, Addressing hard classical problems with Adiabatically Assisted Variational Quantum Eigensolvers (2018), [arXiv:1806.02287 \[quant-ph\]](https://arxiv.org/abs/1806.02287).

[12] M.-C. Chen, M. Gong, X. Xu, X. Yuan, J.-W. Wang, C. Wang, C. Ying, J. Lin, Y. Xu, Y. Wu, S. Wang, H. Deng, F. Liang, C.-Z. Peng, S. C. Benjamin, X. Zhu, C.-Y. Lu, and J.-W. Pan, Demonstration of Adiabatic Variational Quantum Computing with a Superconducting Quantum Coprocessor, *Phys. Rev. Lett.* **125**, 180501 (2020).

[13] N. N. Hegade, K. Paul, Y. Ding, M. Sanz, F. Albarrán-Ariagada, E. Solano, and X. Chen, Shortcuts to Adiabaticity in Digitized Adiabatic Quantum Computing, *Phys. Rev. Appl.* **15**, 024038 (2021).

[14] A. Cervera-Lierta, J. S. Kottmann, and A. Aspuru-Guzik, Meta-Variational Quantum Eigensolver: Learning Energy Profiles of Parameterized Hamiltonians for Quantum Simulation, *PRX Quantum* **2**, 020329 (2021).

[15] Z. Zhan, C. Run, Z. Zong, L. Xiang, Y. Fei, Z. Sun, Y. Wu, Z. Jia, P. Duan, J. Wu, Y. Yin, and G. Guo, Experimental Determination of Electronic States via Digitized Shortcut to Adiabaticity and Sequential Digitized Adiabaticity, *Phys. Rev. Appl.* **16**, 034050 (2021).

[16] S. M. Harwood, D. Trennev, S. T. Stober, P. Barkoutsos, T. P. Gujarati, S. Mostame, and D. Greenberg, Improving the Variational Quantum Eigensolver Using Variational Adiabatic Quantum Computing, *ACM Trans. Quantum Comput.* **3**, 1 (2022).

[17] P. Chandarana, N. N. Hegade, K. Paul, F. Albarrán-Ariagada, E. Solano, A. del Campo, and X. Chen, Digitized-counterdiabatic quantum approximate optimization algorithm, *Phys. Rev. Res.* **4**, 013141 (2022).

[18] B. F. Schiffer, J. Tura, and J. I. Cirac, Adiabatic Spectroscopy and a Variational Quantum Adiabatic Algorithm, *PRX Quantum* **3**, 020347 (2022).

[19] N. N. Hegade, X. Chen, and E. Solano, Digitized counterdiabatic quantum optimization, *Phys. Rev. Res.* **4**, L042030 (2022).

[20] P. Chandarana, P. S. Vieites, N. N. Hegade, E. Solano, Y. Ban, and X. Chen, Meta-learning digitized-counterdiabatic quantum optimization, *Quantum Sci. Technol.* **8**, 045007 (2023).

[21] C. Mc Keever and M. Lubasch, Towards Adiabatic Quantum Computing Using Compressed Quantum Circuits, *PRX Quantum* **5**, 020362 (2024).

[22] I. Kolotouros, I. Petrongonas, M. Prokop, and P. Wallden, Simulating adiabatic quantum computing with parameterized quantum circuits, *Quantum Sci. Technol.* **10**, 015003 (2024).

[23] C. Sanavio, F. Mascherpa, A. Marruzzo, A. Amendola, and S. Succi, Variational-Adiabatic Quantum Solver for Systems of Linear Equations with Warm Starts (2025), [arXiv:2505.24285 \[quant-ph\]](https://arxiv.org/abs/2505.24285).

[24] E. Karacan, C. Mc Keever, M. Foss-Feig, D. Hayes, and M. Lubasch, Filter-enhanced adiabatic quantum computing on a digital quantum processor, *Phys. Rev. Res.* **7**, 033153 (2025).

[25] S. V. Romero, A.-M. Visuri, A. G. Cadavid, A. Simen, E. Solano, and N. N. Hegade, Bias-field digitized counterdiabatic quantum algorithm for higher-order binary optimization, *Commun. Phys.* **8**, 348 (2025).

[26] B. A. Bhargava, S. Kumar, A.-M. Visuri, P. A. Erdman, E. Solano, and N. N. Hegade, Constant Depth Digital-Analog Counterdiabatic Quantum Computing (2026), [arXiv:2601.01154 \[quant-ph\]](https://arxiv.org/abs/2601.01154).

[27] R. Puig, M. Drudis, S. Thanasilp, and Z. Holmes, Variational Quantum Simulation: A Case Study for Understanding Warm Starts, *PRX Quantum* **6**, 010317 (2025).

[28] H. Mhiri, R. Puig, S. Lerch, M. S. Rudolph, T. Chotibut, S. Thanasilp, and Z. Holmes, A unifying account of warm start guarantees for patches of quantum landscapes (2025), [arXiv:2502.07889 \[quant-ph\]](https://arxiv.org/abs/2502.07889).

[29] M. Ballarin, J. J. García-Ripoll, D. Hayes, and M. Lubasch, Efficient quantum state preparation of multivariate functions using tensor networks (2025), [arXiv:2511.15674 \[quant-ph\]](https://arxiv.org/abs/2511.15674).

[30] D. P. Kingma and J. Ba, Adam: A Method for Stochastic Optimization (2017), [arXiv:1412.6980 \[cs.LG\]](https://arxiv.org/abs/1412.6980).

[31] J. Stokes, J. Izaac, N. Killoran, and G. Carleo, Quantum Natural Gradient, *Quantum* **4**, 269 (2020).

[32] See Supplemental Material at [URL will be inserted by publisher] for additional information on the proofs of Theorem 1 and 2, absence of barren plateaus, extension to ϵ -exact representability, and measurement cost and stability under shot noise.

[33] Y. Nesterov, *Lectures on Convex Optimization*, Springer Optimization and Its Applications, Vol. 137 (Springer, Cham, 2018).

[34] L. Hackl, T. Guaita, T. Shi, J. Haegeman, E. Demler, and J. I. Cirac, Geometry of variational methods: dynamics of closed quantum systems, *SciPost Phys.* **9**, 048 (2020).

[35] B. Žunkovič, P. Torta, G. Pecci, G. Lami, and M. Collura, Variational Ground-State Quantum Adiabatic Theorem, *Phys. Rev. Lett.* **134**, 130601 (2025).

[36] T. Kadowaki and H. Nishimori, Quantum annealing in the transverse Ising model, *Phys. Rev. E* **58**, 5355 (1998).

[37] P. Hauke, H. G. Katzgraber, W. Lechner, H. Nishimori, and W. D. Oliver, Perspectives of quantum annealing: methods and implementations, *Rep. Prog. Phys.* **83**, 054401 (2020).

[38] C. Kokail, C. Maier, R. van Bijnen, T. Brydges, M. K. Joshi, P. Jurcevic, C. A. Muschik, P. Silvi, R. Blatt, C. F. Roos, and P. Zoller, Self-verifying variational quantum

simulation of lattice models, [Nature **569**, 355 \(2019\)](#).

[39] Y. Subaşı, R. D. Somma, and D. Orsucci, Quantum Algorithms for Systems of Linear Equations Inspired by Adiabatic Quantum Computing, [Phys. Rev. Lett. **122**, 060504 \(2019\)](#).

[40] P. C. S. Costa, D. An, Y. R. Sanders, Y. Su, R. Babbush, and D. W. Berry, Optimal Scaling Quantum Linear-Systems Solver via Discrete Adiabatic Theorem, [PRX Quantum **3**, 040303 \(2022\)](#).

[41] P. C. S. Costa, D. An, R. Babbush, and D. Berry, The discrete adiabatic quantum linear system solver has lower constant factors than the randomized adiabatic solver, [Quantum **9**, 1887 \(2025\)](#).

[42] R. Puig, B. Casas, A. Cervera-Lierta, Z. Holmes, and A. Pérez-Salinas, Warm Starts, Cold States: Exploiting Adiabaticity for Variational Ground-States (2026), [arXiv:2602.06137 \[quant-ph\]](#).

Supplemental Material:

Scalable, self-verifying variational quantum eigensolver using adiabatic warm starts

Bojan Žunkovič^{1, 2, *} Marco Ballarin^{1, 3} Lewis Wright^{1, 3} and Michael Lubasch^{1, 3, †}

¹University of Ljubljana, Faculty of Computer and Information Science, Večna pot 113, 1000 Ljubljana, Slovenia

²Rudolfovo, Science and Technology Centre, Novo mesto, Slovenia

³Quantinuum, Partnership House, Carlisle Place, London SW1P 1BX, United Kingdom

(Dated: February 19, 2026)

In this supplemental material, we first define the setup and notation. Then we prove both theorems of the main text as well as the absence of barren plateaus. Then we show how to extend our results assuming ϵ -exact representability. Finally, we carry out a detailed shot-noise analysis.

CONTENTS

S1. Setup and notation	1
S2. Proof of Theorem 1: Geometric formulation of adiabatic tracking	3
S3. Proof of Theorem 1: Continuous-time adiabatic formulation and scaling	13
S4. Absence of barren plateaus	21
S5. Proof of Theorem 2: Standard-deviation-based verification	22
S6. Extension to ϵ -exact representability	27
S7. Measurement cost and stability under shot noise	29
References	32

S1. SETUP AND NOTATION

We consider the Hamiltonian

$$H(\lambda) = (1 - \lambda)H_i + \lambda H_f, \quad \lambda \in [0, 1], \quad (\text{S1.1})$$

that interpolates between the initial Hamiltonian H_i and the target final Hamiltonian H_f . We define the instantaneous ground state $|\psi_0(\lambda)\rangle$, spectral gap

$$\Delta(\lambda) = E_1(\lambda) - E_0(\lambda) \quad (\text{S1.2})$$

where $E_0(\lambda)$ ($E_1(\lambda)$) denotes the instantaneous ground (first-excited-state) energy, and minimum spectral gap

$$\Delta_{\min} = \min_{\lambda \in [0, 1]} \Delta(\lambda). \quad (\text{S1.3})$$

A variational family $\{|\psi(\theta)\rangle\}$ is assumed to exactly represent $|\psi_0(\lambda)\rangle$ for all λ . The variational energy is

$$E_\lambda(\theta) = \langle \psi(\theta) | H(\lambda) | \psi(\theta) \rangle, \quad (\text{S1.4})$$

with minimizer $\theta^*(\lambda)$. We assume smooth dependence on λ and bounded operator norms for $H(\lambda)$ and its derivatives.

* bojan.zunkovic@fri.uni-lj.si

† michael.lubasch@quantinuum.com

The local behaviour of the variational landscape can be characterized with the help of the geometric tensor

$$g_{\mu\nu}(\boldsymbol{\theta}(\lambda)) = \text{Re}(\langle \partial_\mu \psi | \partial_\nu \psi \rangle - \langle \partial_\mu \psi | \psi \rangle \langle \psi | \partial_\nu \psi \rangle). \quad (\text{S1.5})$$

We aim to optimize the variational energy in steps. Therefore, we discretize the adiabatic path into T slices,

$$\lambda_t = t \delta\lambda, \quad \delta\lambda = \frac{1}{T}, \quad t = 0, 1, \dots, T, \quad (\text{S1.6})$$

and carry out the optimization iteratively along the path by making use of warm starts. We choose $\boldsymbol{\theta}_0$ to satisfy $|\psi(\boldsymbol{\theta}^*)\rangle = |\psi_0(0)\rangle$. Then, for each slice $t = 1, \dots, T$, we apply a gradient-based optimizer K times to minimize E_{λ_t} using the variational circuit initialized with the previously optimized parameters $\boldsymbol{\theta}_{t-1}$:

$$\boldsymbol{\theta}_t^{(0)} = \boldsymbol{\theta}_{t-1}^{(K)}, \quad (\text{S1.7})$$

$$\boldsymbol{\theta}_t^{(k+1)} = \boldsymbol{\theta}_t^{(k)} - \eta \mathcal{G}_t(\boldsymbol{\theta}_t^{(k)}), \quad k = 0, 1, \dots, K-1,$$

$$|\psi_t\rangle = |\psi(\boldsymbol{\theta}_t^{(K)})\rangle, \quad (\text{S1.8})$$

where $\eta > 0$ is the learning rate and $-\mathcal{G}_t(\boldsymbol{\theta})$ the chosen descent direction at $\lambda = \lambda_t$. For the descent direction, we can use vanilla gradient descent, i.e. $\mathcal{G}_t(\boldsymbol{\theta}) = \nabla_{\boldsymbol{\theta}} E_{\lambda_t}(\boldsymbol{\theta})$, or more advanced gradient-based optimizers. In total, our approach performs $N_{\text{updates}} = TK$ optimization steps.

To obtain our guarantees for **Theorem 1** of the main paper, we use the assumptions:

Assumption 1 (Spectral gap). *The instantaneous ground state of $H(\lambda)$ is nondegenerate and $\Delta_{\min} > 0$.*

Assumption 2 (Exact representability). *For all $\lambda \in [0, 1]$, there exists $\boldsymbol{\theta}^*(\lambda)$ such that*

$$|\psi(\boldsymbol{\theta}^*(\lambda))\rangle = |\psi_0(\lambda)\rangle. \quad (\text{S1.9})$$

Assumption 3 (Nondegenerate geometry). *There exists a constant $\gamma > 0$ such that, for all $\lambda \in [0, 1]$ and all $\boldsymbol{\theta}^*(\lambda)$, the geometric tensor satisfies*

$$\mathbf{g}(\boldsymbol{\theta}^*(\lambda)) \succeq \gamma \mathbb{I}. \quad (\text{S1.10})$$

S1.1. Variational ansatz and derivatives

In the main text and throughout this supplemental material, we utilize a variational ansatz with M parameters over n qubits:

$$|\psi(\boldsymbol{\theta})\rangle = U_{M-1} U_{M-2} \dots U_1 U_0 |0\rangle, \quad U_j = e^{-i P_j \theta_j}, \quad P_j \in \{I, X, Y, Z\}^{\otimes n}. \quad (\text{S1.11})$$

We can express the first derivative of this ansatz as:

$$\frac{\partial |\psi(\boldsymbol{\theta})\rangle}{\partial \theta_k} = U_{M-1} \dots U_{k+1} (-i P_k) U_k \dots U_0 |0\rangle \quad (\text{S1.12})$$

$$= -i U_{M-1} \dots U_{k+1} P_k (U_{M-1} \dots U_{k+1})^\dagger U_{M-1} \dots U_{k+1} U_k \dots U_0 |0\rangle \quad (\text{S1.13})$$

$$= -i \widetilde{P}_k |\psi(\boldsymbol{\theta})\rangle. \quad (\text{S1.14})$$

We thus have a Pauli operator \widetilde{P}_k that is evolved in the Heisenberg picture by all the unitaries that follow it. It is also important to note that \widetilde{P}_k is Hermitian:

$$\widetilde{P}_k = U_{M-1} \dots U_{k+1} P_k (U_{M-1} \dots U_{k+1})^\dagger = \widetilde{P}_k^\dagger. \quad (\text{S1.15})$$

For the second derivative, for $l > k$, we get:

$$\frac{\partial^2 |\psi(\boldsymbol{\theta})\rangle}{\partial \theta_k \partial \theta_l} = U_{M-1} \dots U_{l+1} (-i P_l) U_l \dots U_{k+1} (-i P_k) U_k \dots U_0 |0\rangle \quad (\text{S1.16})$$

$$= -U_{M-1} \dots U_{l+1} P_l (U_{M-1} \dots U_{l+1})^\dagger U_{M-1} \dots U_{l+1} U_l \dots U_{k+1} P_k (U_{M-1} \dots U_{k+1})^\dagger U_{M-1} \dots U_{k+1} U_k \dots U_0 |0\rangle \quad (\text{S1.17})$$

$$= -\widetilde{P}_l \widetilde{P}_k |\psi(\boldsymbol{\theta})\rangle. \quad (\text{S1.18})$$

Note that if $l = k$, the double derivative simplifies to:

$$\frac{\partial^2 |\psi(\boldsymbol{\theta})\rangle}{\partial \theta_k \partial \theta_k} = - |\psi(\boldsymbol{\theta})\rangle. \quad (\text{S1.19})$$

We compute the energy gradients:

$$\frac{\partial \langle H \rangle}{\partial \theta_k} = \frac{\partial \langle \psi(\boldsymbol{\theta}) | H | \psi(\boldsymbol{\theta}) \rangle}{\partial \theta_k} = \frac{\partial \langle \psi(\boldsymbol{\theta}) |}{\partial \theta_k} H |\psi(\boldsymbol{\theta})\rangle + \partial \langle \psi(\boldsymbol{\theta}) | H \frac{|\psi(\boldsymbol{\theta})\rangle}{\partial \theta_k} \quad (\text{S1.20})$$

$$= i \langle \psi(\boldsymbol{\theta}) | \tilde{P}_k H |\psi(\boldsymbol{\theta})\rangle - i \langle \psi(\boldsymbol{\theta}) | H \tilde{P}_k |\psi(\boldsymbol{\theta})\rangle \quad (\text{S1.21})$$

$$= i \langle \psi(\boldsymbol{\theta}) | [\tilde{P}_k, H] |\psi(\boldsymbol{\theta})\rangle \quad (\text{S1.22})$$

$$= 2 \text{Im} \left\{ \langle \psi(\boldsymbol{\theta}) | H \tilde{P}_k |\psi(\boldsymbol{\theta})\rangle \right\}. \quad (\text{S1.23})$$

We compute the off-diagonal elements of the Hessian:

$$\frac{\partial^2 \langle H \rangle}{\partial \theta_k \partial \theta_l} = \frac{\partial^2 \langle \psi(\boldsymbol{\theta}) |}{\partial \theta_k \partial \theta_l} H |\psi(\boldsymbol{\theta})\rangle + \frac{\partial \langle \psi(\boldsymbol{\theta}) |}{\partial \theta_k} H \frac{|\psi(\boldsymbol{\theta})\rangle}{\partial \theta_l} + \frac{\partial \langle \psi(\boldsymbol{\theta}) |}{\partial \theta_l} H \frac{|\psi(\boldsymbol{\theta})\rangle}{\partial \theta_k} + \langle \psi(\boldsymbol{\theta}) | H \frac{\partial^2 |\psi(\boldsymbol{\theta})\rangle}{\partial \theta_k \partial \theta_l} \quad (\text{S1.24})$$

$$= - \langle \psi(\boldsymbol{\theta}) | \tilde{P}_k \tilde{P}_l H |\psi(\boldsymbol{\theta})\rangle + \langle \psi(\boldsymbol{\theta}) | \tilde{P}_k H \tilde{P}_l |\psi(\boldsymbol{\theta})\rangle + \langle \psi(\boldsymbol{\theta}) | \tilde{P}_l H \tilde{P}_k |\psi(\boldsymbol{\theta})\rangle - \langle \psi(\boldsymbol{\theta}) | H \tilde{P}_l \tilde{P}_k |\psi(\boldsymbol{\theta})\rangle \quad (\text{S1.25})$$

$$= \langle \psi(\boldsymbol{\theta}) | [\tilde{P}_k, [H, \tilde{P}_l]] |\psi(\boldsymbol{\theta})\rangle, \quad (\text{S1.26})$$

and the diagonal elements:

$$\frac{\partial^2 \langle H \rangle}{\partial \theta_k \partial \theta_k} = -2 \langle H \rangle + 2 \langle \psi(\boldsymbol{\theta}) | \tilde{P}_k H \tilde{P}_k |\psi(\boldsymbol{\theta})\rangle. \quad (\text{S1.27})$$

Finally, the third derivatives of the energy with respect to the variational parameters read:

$$\frac{\partial^3 \langle H \rangle}{\partial \theta_m \partial \theta_l \partial \theta_k} = -i \left\langle \left[[\tilde{P}_m, \tilde{P}_k], [\tilde{P}_l, H] \right] + \left[[\tilde{P}_k, \tilde{P}_l], [\tilde{P}_m, H] \right] + \left[[\tilde{P}_l, \tilde{P}_m], [\tilde{P}_k, H] \right] \right\rangle_{\boldsymbol{\theta}} \quad (\text{S1.28})$$

S2. PROOF OF THEOREM 1: GEOMETRIC FORMULATION OF ADIABATIC TRACKING

In this section, we establish [Theorem 1](#) of the main text by a sequence of lemmas, based on standard deep-learning techniques, exact smoothness, and Lipschitz bounds arising from the particular choice of the variational ansatz. The algorithm proceeds by first shifting the adiabatic parameter λ by a small amount $\delta\lambda$, ensuring that the previously optimised state lies in a well-behaved region of the new landscape, which guarantees linear convergence to a unique optimum.

Proof roadmap:

- Derivative structure and smoothness.** [Lemma 1](#) gives explicit formulas for the gradient and Hessian for the assumed variational ansatz. The subsequent [Smoothness Lemma 2](#) establishes global L -smoothness, and the [Hessian Lipschitz Lemma 3](#) proves that the Hessian varies in a controlled manner with Lipschitz constant L_H . These lemmas provide bounds on how fast the local optimization landscape properties can change.
- Curvature at the minimum.** The [Hessian lower bound Lemma 4](#) shows that at $\boldsymbol{\theta}^*(\lambda)$ the Hessian is uniformly positive definite, with a lower bound determined by the spectral gap and the nondegeneracy constant of the variational metric. This provides a well-behaved optimization landscape at the variational minimum.
- Local PL inequality** The [Local Polyak–Łojasiewicz Lemma 5](#) combines the curvature lower bound ([Lemma 4](#)) with Hessian Lipschitz continuity ([Lemma 3](#)) to identify a neighborhood in which the PL inequality holds.
- Adiabatic drift and linear contraction** [Lemma 6](#) bounds the drift of the minimizer, i.e., how much $\boldsymbol{\theta}^*(\lambda)$ changes under a change of λ . This can be used together with the [Lemma 5](#) to show linear convergence of the energy error after a sufficiently small step $\delta\lambda$, summarised in the [warm-start Lemma 7](#).
- Tracking error** The [local warm-start Lemma 7](#) and the [adiabatic drift bound Lemma 6](#) are then combined to derive [Theorem 1](#) from the main manuscript. We distinguish two boundary regimes:

- **Option 1:** larger step size $\delta\lambda$ and *many* optimization steps for a fixed λ – discussed in Section S2.2;
- **Option 2:** smaller step size $\delta\lambda$ and only *one* optimization step for a fixed λ – discussed in Section S2.3.

In both cases, we obtain the same scaling of total complexity, with a slightly different resource allocation. In **option 1**, we show that $\delta\lambda \propto \Delta_{\min}^2$ and the number of gradient steps $K \propto 1/\Delta_{\min}$, providing the $1/\Delta_{\min}^3$ scaling. In **option 2**, we take only one gradient update step (i.e., $K = 1$) but have to use more slices, namely $\delta\lambda \propto \Delta_{\min}^3$. Both variants also yield the same total complexity with respect to other physical parameters, but differ slightly in their numerical constants. **Theorem 1** of the main text is for simplicity structured to be in line with the **option 1**, but it could equally well be written in terms of the **option 2**.

S2.1. Lemmas and linear convergence theorem

Lemma 1 (Derivatives). *The gradient and Hessian satisfy*

$$\partial_{\theta_k} E(\boldsymbol{\theta}) = i\langle\psi|[\tilde{P}_k, H]|\psi\rangle, \quad (\text{S2.29})$$

$$\partial_{\theta_k} \partial_{\theta_l} E(\boldsymbol{\theta}) = \langle\psi|[\tilde{P}_k, [H, \tilde{P}_l]]|\psi\rangle, \quad (\text{S2.30})$$

where \tilde{P}_k denotes the conjugate generator.

Proof. These expressions were proven in Section S1.1. \square

Lemma 2 (Smoothness). *The energy $E_\lambda(\boldsymbol{\theta})$ is L -smooth with*

$$L = \sup_{\boldsymbol{\theta}} \|\nabla^2 E(\boldsymbol{\theta})\|_{\text{op}} \leq 4\|H\|_{\text{op}}M. \quad (\text{S2.31})$$

Proof. From Lemma 1, the Hessian entries are given by

$$\partial_{\theta_k} \partial_{\theta_l} E(\boldsymbol{\theta}) = \langle\psi(\boldsymbol{\theta})|[\tilde{P}_k, [H, \tilde{P}_l]]|\psi(\boldsymbol{\theta})\rangle, \quad (\text{S2.32})$$

where $\tilde{P}_k = U_{>k} P_k U_{>k}^{\text{opt}}$ denotes the conjugated generator. As \tilde{P}_k is Hermitian and unitary, hence $\|\tilde{P}_k\|_{\text{op}} = 1$. To bound the operator norm of the Hessian, we use the variational characterization

$$\|\nabla^2 E(\boldsymbol{\theta})\|_{\text{op}} = \sup_{\|v\|_2=1} |v^\top \nabla^2 E(\boldsymbol{\theta}) v|. \quad (\text{S2.33})$$

For any $v \in \mathbb{R}^M$ with $\|v\|_2 = 1$, define the operator

$$A(v) = \sum_{k=1}^M v_k \tilde{P}_k. \quad (\text{S2.34})$$

Using the bilinearity of the Hessian, we obtain

$$v^\top \nabla^2 E(\boldsymbol{\theta}) v = \sum_{k,l} v_k v_l \langle\psi|[\tilde{P}_k, [H, \tilde{P}_l]]|\psi\rangle \quad (\text{S2.35})$$

$$= \langle\psi|[A(v), [H, A(v)]]|\psi\rangle. \quad (\text{S2.36})$$

Taking the absolute value and using that expectation values are bounded by the operator norm yields

$$|\langle\psi|[A(v), [H, A(v)]]|\psi\rangle| \leq \| [A(v), [H, A(v)]] \|_{\text{op}}. \quad (\text{S2.37})$$

We now bound the double commutator using the general inequality $\|[X, Y]\|_{\text{op}} \leq 2\|X\|_{\text{op}}\|Y\|_{\text{op}}$:

$$\|[A, [H, A]]\|_{\text{op}} \leq 2\|A\|_{\text{op}}\|[H, A]\|_{\text{op}} \quad (\text{S2.38})$$

$$\leq 2\|A\|_{\text{op}} \cdot 2\|H\|_{\text{op}}\|A\|_{\text{op}} = 4\|H\|_{\text{op}}\|A\|_{\text{op}}^2. \quad (\text{S2.39})$$

It remains to bound $\|A(v)\|_{\text{op}}$. Since each \tilde{P}_k is unitary,

$$\|A(v)\|_{\text{op}} \leq \sum_{k=1}^M |v_k| \|\tilde{P}_k\|_{\text{op}} \quad (\text{S2.40})$$

$$= \sum_{k=1}^M |v_k| \leq \|v\|_1 \leq \sqrt{M} \|v\|_2. \quad (\text{S2.41})$$

For $\|v\|_2 = 1$, this implies

$$\|A(v)\|_{\text{op}}^2 \leq M. \quad (\text{S2.42})$$

Combining the above bounds, we conclude that for all unit vectors v ,

$$|v^\top \nabla^2 E(\boldsymbol{\theta}) v| \leq 4\|H\|_{\text{op}} M. \quad (\text{S2.43})$$

Taking the supremum over v yields

$$\|\nabla^2 E(\boldsymbol{\theta})\|_{\text{op}} \leq 4\|H\|_{\text{op}} M, \quad (\text{S2.44})$$

uniformly in $\boldsymbol{\theta}$. \square

Lemma 3 (Hessian Lipschitz continuity). *For all $\boldsymbol{\theta}, \boldsymbol{\theta}' \in \mathbb{R}^M$, the Hessian of the variational energy satisfies*

$$\|\nabla^2 E(\boldsymbol{\theta}') - \nabla^2 E(\boldsymbol{\theta})\|_{\text{op}} \leq L_H \|\boldsymbol{\theta}' - \boldsymbol{\theta}\|_2, \quad (\text{S2.45})$$

with Lipschitz constant

$$L_H = 24\|H\|_{\text{op}} M^{3/2}. \quad (\text{S2.46})$$

Proof. We interpolate linearly between the two parameter points by defining

$$\boldsymbol{\theta}(t) = \boldsymbol{\theta} + t(\boldsymbol{\theta}' - \boldsymbol{\theta}), \quad (\text{S2.47})$$

with $t \in [0, 1]$. By the fundamental theorem of calculus,

$$\nabla^2 E(\boldsymbol{\theta}') - \nabla^2 E(\boldsymbol{\theta}) = \int_0^1 \frac{d}{dt} \nabla^2 E(\boldsymbol{\theta}(t)) dt. \quad (\text{S2.48})$$

Taking the operator norm and applying the triangle inequality yields

$$\|\nabla^2 E(\boldsymbol{\theta}') - \nabla^2 E(\boldsymbol{\theta})\|_{\text{op}} \leq \int_0^1 \left\| \frac{d}{dt} \nabla^2 E(\boldsymbol{\theta}(t)) \right\|_{\text{op}} dt. \quad (\text{S2.49})$$

The derivative of the Hessian along the path can be written using the chain rule as

$$\frac{d}{dt} \nabla^2 E(\boldsymbol{\theta}(t)) = \sum_{m=1}^M (\boldsymbol{\theta}'_m - \boldsymbol{\theta}_m) \nabla_m^3 E(\boldsymbol{\theta}(t)). \quad (\text{S2.50})$$

Taking norms gives

$$\left\| \frac{d}{dt} \nabla^2 E(\boldsymbol{\theta}(t)) \right\|_{\text{op}} \leq \sum_{m=1}^M |\boldsymbol{\theta}'_m - \boldsymbol{\theta}_m| \|\nabla_m^3 E(\boldsymbol{\theta}(t))\|_{\text{op}}. \quad (\text{S2.51})$$

Applying Cauchy–Schwarz to the sum over m produces the first \sqrt{M} factor:

$$\sum_{m=1}^M |\boldsymbol{\theta}'_m - \boldsymbol{\theta}_m| \leq \sqrt{M} \|\boldsymbol{\theta}' - \boldsymbol{\theta}\|_2. \quad (\text{S2.52})$$

Hence,

$$\left\| \frac{d}{dt} \nabla^2 E(\boldsymbol{\theta}(t)) \right\|_{\text{op}} \leq \sqrt{M} \|\boldsymbol{\theta}' - \boldsymbol{\theta}\|_2 \max_m \|\nabla_m^3 E(\boldsymbol{\theta}(t))\|_{\text{op}}. \quad (\text{S2.53})$$

We now bound $\|\nabla_m^3 E(\boldsymbol{\theta})\|_{\text{op}}$. From the explicit third-derivative formula, each component has the structure

$$\partial_{\theta_m} \partial_{\theta_k} \partial_{\theta_l} E(\boldsymbol{\theta}) = \langle \psi | [[\tilde{P}_m, \tilde{P}_k], [\tilde{P}_l, H]] | \psi \rangle + \text{permutations}. \quad (\text{S2.54})$$

The operator norm of $\nabla_m^3 E$ is obtained by taking the supremum over unit vectors $u, v \in \mathbb{R}^M$:

$$\|\nabla_m^3 E(\boldsymbol{\theta})\|_{\text{op}} = \sup_{\|u\|_2 = \|v\|_2 = 1} \left| \sum_{k,l=1}^M u_k v_l \partial_{\theta_m} \partial_{\theta_k} \partial_{\theta_l} E(\boldsymbol{\theta}) \right|. \quad (\text{S2.55})$$

Using Cauchy–Schwarz twice yields the second source of M :

$$\sum_{k,l=1}^M |u_k| |v_l| \leq \|u\|_1 \|v\|_1 \leq M. \quad (\text{S2.56})$$

Each nested commutator term satisfies

$$\|[[\tilde{P}_m, \tilde{P}_k], [\tilde{P}_l, H]]\|_{\text{op}} \leq 8\|H\|_{\text{op}}, \quad (\text{S2.57})$$

since $\|\tilde{P}_j\|_{\text{op}} = 1$ and $\|[X, Y]\|_{\text{op}} \leq 2\|X\|_{\text{op}}\|Y\|_{\text{op}}$. Accounting for the three permutations appearing in the third derivative gives

$$\|\nabla_m^3 E(\boldsymbol{\theta})\|_{\text{op}} \leq 24\|H\|_{\text{op}} M. \quad (\text{S2.58})$$

Substituting this bound back, we obtain

$$\left\| \frac{d}{dt} \nabla^2 E(\boldsymbol{\theta}(t)) \right\|_{\text{op}} \leq 24\|H\|_{\text{op}} M^{3/2} \|\boldsymbol{\theta}' - \boldsymbol{\theta}\|_2. \quad (\text{S2.59})$$

Finally, integrating over $t \in [0, 1]$ yields

$$\|\nabla^2 E(\boldsymbol{\theta}') - \nabla^2 E(\boldsymbol{\theta})\|_{\text{op}} \leq 24\|H\|_{\text{op}} M^{3/2} \|\boldsymbol{\theta}' - \boldsymbol{\theta}\|_2. \quad (\text{S2.60})$$

□

Lemma 4 (Hessian lower bound). *At the variational minimum $\boldsymbol{\theta}^*(\lambda)$, the Hessian of the energy satisfies*

$$\nabla^2 E_{\lambda}(\boldsymbol{\theta}^*(\lambda)) \succeq 2\gamma \Delta_{\min} I. \quad (\text{S2.61})$$

Proof. We evaluate the Hessian at the variational minimum $\boldsymbol{\theta}^*$ where $|\psi(\boldsymbol{\theta}^*)\rangle = |0\rangle$ is the nondegenerate ground state of $H(\lambda)$ with eigenvalue E_0 . Let $v \in \mathbb{R}^M$ be an arbitrary unit vector with $\|v\|_2 = 1$.

Using the Hessian formula from Lemma 1, we write the quadratic form as

$$v^{\top} \nabla^2 E(\boldsymbol{\theta}^*) v = \sum_{k,l=1}^M v_k v_l \langle 0 | [\tilde{P}_k, [H, \tilde{P}_l]] | 0 \rangle. \quad (\text{S2.62})$$

Define the operator $A(v) = \sum_{k=1}^M v_k \tilde{P}_k$. By bilinearity of the commutator, this yields

$$v^{\top} \nabla^2 E(\boldsymbol{\theta}^*) v = \langle 0 | [A(v), [H, A(v)]] | 0 \rangle. \quad (\text{S2.63})$$

Using the identity $[A, [H, A]] = 2A(H - E_0)A - \{A^2, (H - E_0)\}$ and the fact that $(H - E_0)|0\rangle = 0$, the second term vanishes in the expectation value, leaving

$$\langle 0 | [A, [H, A]] | 0 \rangle = 2\langle 0 | A(H - E_0)A | 0 \rangle. \quad (\text{S2.64})$$

We insert a complete set of energy eigenstates $\{|n\rangle\}_{n \geq 0}$. Since the term for $n = 0$ vanishes (as $E_0 - E_0 = 0$), the sum restricts to the excited subspace:

$$2\langle 0|A(H - E_0)A|0\rangle = 2 \sum_{n \geq 1} (E_n - E_0) |\langle n|A|0\rangle|^2. \quad (\text{S2.65})$$

Using the uniform spectral gap assumption $E_n - E_0 \geq \Delta_{\min}$ for all $n \geq 1$, we obtain:

$$v^\top \nabla^2 E(\boldsymbol{\theta}^*) v \geq 2\Delta_{\min} \sum_{n \geq 1} |\langle n|A|0\rangle|^2 \quad (\text{S2.66})$$

$$= 2\Delta_{\min} \left(\sum_{n \geq 0} |\langle n|A|0\rangle|^2 - |\langle 0|A|0\rangle|^2 \right) \quad (\text{S2.67})$$

$$= 2\Delta_{\min} (\langle 0|A^2|0\rangle - \langle 0|A|0\rangle^2). \quad (\text{S2.68})$$

The term in the parentheses is exactly the variance of the operator A with respect to the ground state. This corresponds to the Fubini-Study metric, which projects the derivatives onto the tangent space orthogonal to $|0\rangle$:

$$\text{Var}(A) = \sum_{k,l} v_k v_l \left(\langle 0|\tilde{P}_k \tilde{P}_l|0\rangle - \langle 0|\tilde{P}_k|0\rangle \langle 0|\tilde{P}_l|0\rangle \right) = v^\top \mathbf{g}(\boldsymbol{\theta}^*) v. \quad (\text{S2.69})$$

By assumption, the ansatz is non-degenerate such that $\mathbf{g}(\boldsymbol{\theta}^*) \succeq \gamma I$, which implies $v^\top \mathbf{g}(\boldsymbol{\theta}^*) v \geq \gamma$. Therefore:

$$v^\top \nabla^2 E(\boldsymbol{\theta}^*) v \geq 2\gamma\Delta_{\min}. \quad (\text{S2.70})$$

Since this bound holds for all unit vectors v , we conclude

$$\nabla^2 E(\boldsymbol{\theta}^*) \succeq 2\gamma\Delta_{\min} I. \quad (\text{S2.71})$$

□

Lemma 5 (Local Polyak–Łojasiewicz inequality). *Let $\boldsymbol{\theta}^*$ denote the variational minimum at fixed λ . For*

$$\|\boldsymbol{\theta} - \boldsymbol{\theta}^*\|_2 \leq r_{\text{PL}} = \frac{\gamma\Delta_{\min}}{L_H}, \quad (\text{S2.72})$$

the Polyak–Łojasiewicz inequality holds:

$$\frac{1}{2} \|\nabla E(\boldsymbol{\theta})\|_2^2 \geq \gamma\Delta_{\min} (E(\boldsymbol{\theta}) - E(\boldsymbol{\theta}^*)). \quad (\text{S2.73})$$

Proof. We begin by recalling from Lemma 4 that the Hessian at the minimum satisfies

$$\nabla^2 E(\boldsymbol{\theta}^*) \succeq 2\gamma\Delta_{\min} I. \quad (\text{S2.74})$$

By Lemma 3, the Hessian is Lipschitz continuous with constant L_H , meaning

$$\|\nabla^2 E(\boldsymbol{\theta}) - \nabla^2 E(\boldsymbol{\theta}^*)\|_{\text{op}} \leq L_H \|\boldsymbol{\theta} - \boldsymbol{\theta}^*\|_2. \quad (\text{S2.75})$$

Since the Hessian is symmetric, we obtain a lower bound $\boldsymbol{\theta}$:

$$\nabla^2 E(\boldsymbol{\theta}) \succeq \nabla^2 E(\boldsymbol{\theta}^*) - \|\nabla^2 E(\boldsymbol{\theta}) - \nabla^2 E(\boldsymbol{\theta}^*)\|_{\text{op}} I. \quad (\text{S2.76})$$

Substituting the previous bounds yields

$$\nabla^2 E(\boldsymbol{\theta}) \succeq (2\gamma\Delta_{\min} - L_H \|\boldsymbol{\theta} - \boldsymbol{\theta}^*\|_2) I. \quad (\text{S2.77})$$

If $\|\boldsymbol{\theta} - \boldsymbol{\theta}^*\|_2 \leq \gamma\Delta_{\min}/L_H$, then

$$2\gamma\Delta_{\min} - L_H \|\boldsymbol{\theta} - \boldsymbol{\theta}^*\|_2 \geq \gamma\Delta_{\min}, \quad (\text{S2.78})$$

and hence

$$\nabla^2 E(\boldsymbol{\theta}) \succeq \gamma \Delta_{\min} I. \quad (\text{S2.79})$$

Therefore, the energy is $\gamma \Delta_{\min}$ -strongly convex in this neighborhood. Strong convexity implies the following quadratic lower bound on the function:

$$E(\boldsymbol{\theta}) - E(\boldsymbol{\theta}^*) \leq \frac{1}{2\gamma \Delta_{\min}} \|\nabla E(\boldsymbol{\theta})\|_2^2. \quad (\text{S2.80})$$

Rearranging this inequality yields

$$\frac{1}{2} \|\nabla E(\boldsymbol{\theta})\|_2^2 \geq \gamma \Delta_{\min} (E(\boldsymbol{\theta}) - E(\boldsymbol{\theta}^*)), \quad (\text{S2.81})$$

which is exactly the Polyak–Lojasiewicz inequality. Since all steps hold whenever $\|\boldsymbol{\theta} - \boldsymbol{\theta}^*\|_2 \leq r_{\text{PL}}$, the claim follows. \square

Lemma 6 (Drift bound). *Let $\boldsymbol{\theta}^*(\lambda)$ denote the variational minimizer of*

$$E_\lambda(\boldsymbol{\theta}) = \langle \psi(\boldsymbol{\theta}) | H(\lambda) | \psi(\boldsymbol{\theta}) \rangle. \quad (\text{S2.82})$$

Assume that the Hessian at the minimum satisfies

$$\nabla_{\boldsymbol{\theta}}^2 E_\lambda(\boldsymbol{\theta}^*(\lambda)) \succeq 2\gamma \Delta_{\min} I, \quad (\text{S2.83})$$

and that $\|\tilde{P}_k\|_{\text{op}} = 1$ for all generators. Then, for sufficiently small $\delta\lambda$,

$$\|\boldsymbol{\theta}^*(\lambda + \delta\lambda) - \boldsymbol{\theta}^*(\lambda)\|_2 \leq D\delta\lambda + O(\delta\lambda^2), \quad D = \frac{\sqrt{M} \|\partial_\lambda H(\lambda)\|_{\text{op}}}{\gamma \Delta_{\min}}. \quad (\text{S2.84})$$

Proof. At the variational minimum, the gradient vanishes:

$$\nabla_{\boldsymbol{\theta}} E_\lambda(\boldsymbol{\theta}^*(\lambda)) = 0. \quad (\text{S2.85})$$

Differentiating with respect to λ gives

$$\frac{d}{d\lambda} \nabla_{\boldsymbol{\theta}} E_\lambda(\boldsymbol{\theta}^*(\lambda)) = 0. \quad (\text{S2.86})$$

Applying the chain rule yields

$$\nabla_{\boldsymbol{\theta}}^2 E_\lambda(\boldsymbol{\theta}^*(\lambda)) \dot{\boldsymbol{\theta}}^*(\lambda) + \nabla_{\boldsymbol{\theta}} \partial_\lambda E_\lambda(\boldsymbol{\theta}^*(\lambda)) = 0, \quad (\text{S2.87})$$

where

$$\dot{\boldsymbol{\theta}}^*(\lambda) = \frac{d}{d\lambda} \boldsymbol{\theta}^*(\lambda). \quad (\text{S2.88})$$

Rearranging,

$$\dot{\boldsymbol{\theta}}^*(\lambda) = -(\nabla_{\boldsymbol{\theta}}^2 E_\lambda(\boldsymbol{\theta}^*(\lambda)))^{-1} \nabla_{\boldsymbol{\theta}} \partial_\lambda E_\lambda(\boldsymbol{\theta}^*(\lambda)). \quad (\text{S2.89})$$

We first bound the inverse Hessian. From the assumed curvature lower bound,

$$\nabla_{\boldsymbol{\theta}}^2 E_\lambda(\boldsymbol{\theta}^*(\lambda)) \succeq 2\gamma \Delta_{\min} I, \quad (\text{S2.90})$$

it follows that

$$\|(\nabla_{\boldsymbol{\theta}}^2 E_\lambda(\boldsymbol{\theta}^*(\lambda)))^{-1}\|_{\text{op}} \leq \frac{1}{2\gamma \Delta_{\min}}. \quad (\text{S2.91})$$

Next, we bound the gradient $\nabla_{\boldsymbol{\theta}} \partial_\lambda E_\lambda$. By definition,

$$\partial_\lambda E_\lambda(\boldsymbol{\theta}) = \langle \psi(\boldsymbol{\theta}) | \partial_\lambda H(\lambda) | \psi(\boldsymbol{\theta}) \rangle. \quad (\text{S2.92})$$

Differentiating with respect to θ_k yields

$$\partial_{\theta_k} \partial_\lambda E_\lambda(\boldsymbol{\theta}) = i \langle \psi(\boldsymbol{\theta}) | [\tilde{P}_k, \partial_\lambda H(\lambda)] | \psi(\boldsymbol{\theta}) \rangle. \quad (\text{S2.93})$$

Using the commutator norm bound gives

$$|\partial_{\theta_k} \partial_\lambda E_\lambda(\boldsymbol{\theta})| \leq 2 \|\partial_\lambda H(\lambda)\|_{\text{op}}. \quad (\text{S2.94})$$

Therefore, the Euclidean norm of the gradient satisfies

$$\|\nabla_{\boldsymbol{\theta}} \partial_\lambda E_\lambda(\boldsymbol{\theta}^*(\lambda))\|_2 = \left(\sum_{k=1}^M |\partial_{\theta_k} \partial_\lambda E_\lambda|^2 \right)^{1/2} \leq 2\sqrt{M} \|\partial_\lambda H(\lambda)\|_{\text{op}}. \quad (\text{S2.95})$$

Combining the bounds yields

$$\|\dot{\boldsymbol{\theta}}^*(\lambda)\|_2 \leq \frac{1}{2\gamma\Delta_{\min}} \|\nabla_{\boldsymbol{\theta}} \partial_\lambda E_\lambda(\boldsymbol{\theta}^*(\lambda))\|_2 \leq \frac{\sqrt{M} \|\partial_\lambda H(\lambda)\|_{\text{op}}}{\gamma\Delta_{\min}}. \quad (\text{S2.96})$$

Finally, integrating over $\lambda \in [\lambda, \lambda + \delta\lambda]$ gives (since the assumed adiabatic schedule is linear in λ)

$$\|\boldsymbol{\theta}^*(\lambda + \delta\lambda) - \boldsymbol{\theta}^*(\lambda)\|_2 \leq \frac{\sqrt{M} \|\partial_\lambda H(\lambda)\|_{\text{op}}}{\gamma\Delta_{\min}} \delta\lambda, \quad (\text{S2.97})$$

which proves the claim. \square

Lemma 7 (Adiabatic warm-start convergence). *Let*

$$H(\lambda) = (1 - \lambda)H_i + \lambda H_f, \quad \lambda \in [0, 1], \quad (\text{S2.98})$$

and let

$$E_\lambda(\boldsymbol{\theta}) = \langle \psi(\boldsymbol{\theta}) | H(\lambda) | \psi(\boldsymbol{\theta}) \rangle \quad (\text{S2.99})$$

with a parametrized ansatz $|\psi(\boldsymbol{\theta})\rangle$ that exactly represents the ground state:

$$|\psi(\boldsymbol{\theta}^*(\lambda))\rangle = |\psi_0(\lambda)\rangle. \quad (\text{S2.100})$$

Assume only:

$$E_1(\lambda) - E_0(\lambda) \geq \Delta_{\min} > 0 \quad \forall \lambda, \quad (\text{S2.101})$$

$$\mathbf{g}(\boldsymbol{\theta}^*(\lambda)) \succeq \gamma I. \quad (\text{S2.102})$$

Then there exists an explicit constant $c > 0$ such that, if

$$\delta\lambda \leq c \frac{\gamma^2 \Delta_{\min}^2}{L_H \sqrt{M} \|\partial_\lambda H(\lambda)\|_{\text{op}}}, \quad (\text{S2.103})$$

the minimizer $\boldsymbol{\theta}^*(\lambda)$ lies in a Polyak–Lojasiewicz (PL) region of $E_{\lambda+\delta\lambda}$.

Within this region, gradient descent with step size $\eta \leq 1/L$ converges linearly both in energy and in parameters:

$$E_{\lambda+\delta\lambda}(\boldsymbol{\theta}^{(k)}) - E_{\lambda+\delta\lambda}(\boldsymbol{\theta}^*) \leq \left(1 - \frac{\gamma\Delta_{\min}}{L}\right)^k \delta E_0, \quad (\text{S2.104})$$

$$\|\boldsymbol{\theta}^{(k)} - \boldsymbol{\theta}^*(\lambda + \delta\lambda)\|_2 \leq \left(1 - \frac{\gamma\Delta_{\min}}{L}\right)^{k/2} \|\boldsymbol{\theta}^{(0)} - \boldsymbol{\theta}^*(\lambda + \delta\lambda)\|_2. \quad (\text{S2.105})$$

In particular, to reach energy accuracy ϵ , it suffices that the total number of optimization steps K is

$$K \geq \frac{L}{\gamma\Delta_{\min}} \ln \left(\frac{\delta E_0}{\epsilon} \right), \quad (\text{S2.106})$$

and the corresponding parameter error satisfies

$$\|\boldsymbol{\theta}^{(K)} - \boldsymbol{\theta}^*(\lambda + \delta\lambda)\|_2 \leq \sqrt{\frac{2\epsilon}{\gamma\Delta_{\min}}}. \quad (\text{S2.107})$$

Proof. At $\boldsymbol{\theta}^*(\lambda)$ the gradient vanishes:

$$\nabla_{\boldsymbol{\theta}} E_{\lambda}(\boldsymbol{\theta}^*(\lambda)) = 0. \quad (\text{S2.108})$$

From Lemma 6,

$$\|\boldsymbol{\theta}^*(\lambda + \delta\lambda) - \boldsymbol{\theta}^*(\lambda)\|_2 \leq \frac{\sqrt{M} \|\partial_{\lambda} H(\lambda)\|_{\text{op}}}{\gamma \Delta_{\min}} \delta\lambda. \quad (\text{S2.109})$$

Requiring this drift to be bounded by the PL radius $r_{\text{PL}} = \gamma \Delta_{\min} / L_H$ yields the stated condition on $\delta\lambda$.

Inside the PL region, the energy is $\gamma \Delta_{\min}$ -strongly convex and L -smooth. For one gradient descent step with $\eta = 1/L$ we have by the gradient descent lemma [1],

$$E(\boldsymbol{\theta}^{(k+1)}) \leq E(\boldsymbol{\theta}^{(k)}) - \frac{1}{2L} \|\nabla E(\boldsymbol{\theta}^{(k)})\|_2^2. \quad (\text{S2.110})$$

Applying the PL inequality

$$\frac{1}{2} \|\nabla E(\boldsymbol{\theta})\|_2^2 \geq \gamma \Delta_{\min} (E(\boldsymbol{\theta}) - E(\boldsymbol{\theta}^*)), \quad (\text{S2.111})$$

and defining $\delta E_k = E(\boldsymbol{\theta}^{(k)}) - E(\boldsymbol{\theta}^*)$ gives

$$\delta E_{k+1} \leq \left(1 - \frac{\gamma \Delta_{\min}}{L}\right) \delta E_k. \quad (\text{S2.112})$$

Iterating yields

$$\delta E_k \leq \left(1 - \frac{\gamma \Delta_{\min}}{L}\right)^k \delta E_0 \leq e^{-k \frac{\gamma \Delta_{\min}}{L}} \delta E_0. \quad (\text{S2.113})$$

Strong convexity additionally implies

$$\frac{\gamma \Delta_{\min}}{2} \|\boldsymbol{\theta} - \boldsymbol{\theta}^*\|_2^2 \leq E(\boldsymbol{\theta}) - E(\boldsymbol{\theta}^*). \quad (\text{S2.114})$$

Combining with the energy decay gives

$$\|\boldsymbol{\theta}^{(k)} - \boldsymbol{\theta}^*\|_2^2 \leq \frac{2}{\gamma \Delta_{\min}} \delta E_k \leq \frac{2}{\gamma \Delta_{\min}} \left(1 - \frac{\gamma \Delta_{\min}}{L}\right)^k \delta E_0, \quad (\text{S2.115})$$

which yields linear convergence in parameters and the stated bound. \square

S2.2. Ground state tracking — option 1

Discretization condition

We discretize λ so that consecutive minimizers lie within half of the PL radius:

$$\|\boldsymbol{\theta}^*(\lambda_{k+1}) - \boldsymbol{\theta}^*(\lambda_k)\|_2 \leq \frac{r_{\text{PL}}}{2}. \quad (\text{S2.116})$$

This is ensured provided

$$\delta\lambda \leq \frac{\gamma \Delta_{\min}}{2\sqrt{M} \|\partial_{\lambda} H\|_{\text{op}}} r_{\text{PL}} = \frac{\gamma^2 \Delta_{\min}^2}{2L_H \sqrt{M} \|\partial_{\lambda} H\|_{\text{op}}}. \quad (\text{S2.117})$$

Warm-start entry into the PL region

Assume that at step t the iterate satisfies

$$\|\boldsymbol{\theta}_t - \boldsymbol{\theta}^*(\lambda_t)\|_2 \leq \frac{r_{\text{PL}}}{2}. \quad (\text{S2.118})$$

Then, using the triangle inequality,

$$\|\boldsymbol{\theta}_t - \boldsymbol{\theta}^*(\lambda_{t+1})\|_2 \leq \|\boldsymbol{\theta}_t - \boldsymbol{\theta}^*(\lambda_t)\|_2 + \|\boldsymbol{\theta}^*(\lambda_t) - \boldsymbol{\theta}^*(\lambda_{t+1})\|_2 \quad (\text{S2.119})$$

$$\leq \frac{r_{\text{PL}}}{2} + \frac{r_{\text{PL}}}{2} = r_{\text{PL}}. \quad (\text{S2.120})$$

Hence, the warm start always lies inside the PL region of the next energy landscape.

Gradient descent contraction

Inside the PL region, by the Lemma 7 the gradient descent with step size $\eta = 1/L$ satisfies

$$\|\boldsymbol{\theta}^{(k+1)} - \boldsymbol{\theta}^*\|_2 \leq \sqrt{1 - \frac{\gamma \Delta_{\min}}{L}} \|\boldsymbol{\theta}^{(k)} - \boldsymbol{\theta}^*\|_2. \quad (\text{S2.121})$$

To reduce the error by a factor of 2, i.e.

$$\|\boldsymbol{\theta}^{(k)} - \boldsymbol{\theta}^*\|_2 \leq \frac{r_{\text{PL}}}{2}, \quad (\text{S2.122})$$

it suffices to choose t such that

$$\left(1 - \frac{\gamma \Delta_{\min}}{L}\right)^{k/2} \leq \frac{1}{2}. \quad (\text{S2.123})$$

Using $\ln(1 - x) \leq -x$ for $x \in (0, 1)$, we obtain

$$k \geq K = \frac{2L}{\gamma \Delta_{\min}} \ln 2. \quad (\text{S2.124})$$

Total complexity

The total number of adiabatic steps is

$$T = \frac{1}{\delta \lambda} = \frac{2L_H \sqrt{M} \|\partial_\lambda H\|_{\text{op}}}{\gamma^2 \Delta_{\min}^2}. \quad (\text{S2.125})$$

At each step, we perform K gradient descent iterations as in (S2.124). Therefore, the total number of gradient evaluations satisfies

$$N_{\text{grad}} = T \cdot K \quad (\text{S2.126})$$

$$= \frac{4L_H \sqrt{M} \|\partial_\lambda H\|_{\text{op}}}{\gamma^2 \Delta_{\min}^2} \cdot \frac{L}{\gamma \Delta_{\min}} \ln 2. \quad (\text{S2.127})$$

Substituting $L \leq 4\|H\|_{\text{op}}M$, we finally obtain

$$N_{\text{updates}} \leq \frac{16 \ln 2}{\gamma^3} \frac{L_H \|H\|_{\text{op}} M^{3/2} \|\partial_\lambda H\|_{\text{op}}}{\Delta_{\min}^3}. \quad (\text{S2.128})$$

Inserting all constants, we find

$$N_{\text{updates}} \leq 384 \ln 2 \frac{M^3 \|H\|_{\text{op}}^2 \|H_f - H_i\|_{\text{op}}}{\gamma^3 \Delta_{\min}^3}$$

(S2.129)

This is the protocol used in **Theorem 1** of the main manuscript. An alternative version is presented in the following subsection.

S2.3. Ground state tracking — option 2

In this section, we refine the warm-start analysis of Section S2.2 by explicitly tracking the *transient optimization error* across adiabatic steps. Rather than requiring near-exact re-optimization at each step, we show that finite optimization effort per step suffices: the tracking error obeys a contractive recursion with an $\mathcal{O}(\delta\lambda)$ forcing term, yielding a uniform steady-state bound. In the end, we achieve the same level of optimization complexity with a slightly different analysis.

Forced contraction recursion

We decompose the error after the k -th step:

$$e_{t+1} = \boldsymbol{\theta}^{(k=0)} - \boldsymbol{\theta}^*(\lambda_{t+1}) \quad (\text{S2.130})$$

$$= (\boldsymbol{\theta}^{(k=0)} - \boldsymbol{\theta}^*(\lambda_{t+1})) - (\boldsymbol{\theta}^*(\lambda_{t+1}) - \boldsymbol{\theta}^*(\lambda_t)). \quad (\text{S2.131})$$

By Lemma 7, starting from $\boldsymbol{\theta}^{(k=0)}$ and optimizing $E_{\lambda_{t+1}}$ for K steps yields

$$\|\boldsymbol{\theta}^{(k=K)} - \boldsymbol{\theta}^*(\lambda_{t+1})\|_2 \leq \rho^K \|\boldsymbol{\theta}^{(k=0)} - \boldsymbol{\theta}^*(\lambda_{t+1})\|_2, \quad \rho = \sqrt{1 - \frac{\gamma\Delta_{\min}}{2}}. \quad (\text{S2.132})$$

Using the triangle inequality and the drift bound,

$$\|\boldsymbol{\theta}_t^{(k=0)} - \boldsymbol{\theta}^*(\lambda_{t+1})\|_2 \leq \|\boldsymbol{\theta}^{(k=0)} - \boldsymbol{\theta}^*(\lambda_t)\|_2 + \|\boldsymbol{\theta}^*(\lambda_{t+1}) - \boldsymbol{\theta}^*(\lambda_t)\|_2 \quad (\text{S2.133})$$

$$\leq \|e_t\|_2 + D\delta\lambda + O(\delta\lambda^2). \quad (\text{S2.134})$$

Combining the last two inequalities, we find

$$\|e_{t+1}\|_2 \leq \rho^K \|e_t\|_2 + \rho^K D\delta\lambda + O(\delta\lambda^2). \quad (\text{S2.135})$$

Uniform tracking error

Iterating the recursion of Eq. S2.135 gives

$$\|e_t\|_2 \leq (\rho^K)^t \|e_0\|_2 + \rho^K D\delta\lambda \sum_{j=0}^{t-1} (\rho^K)^j + O(\delta\lambda^2) \quad (\text{S2.136})$$

$$\leq (\rho^K)^t \|e_0\|_2 + \frac{\rho^K}{1 - \rho^K} D\delta\lambda + O(\delta\lambda^2). \quad (\text{S2.137})$$

Since $1 - \rho^K \approx K\gamma\Delta_{\min}/2L$ for small $\gamma\Delta_{\min}/L$ we find

$$\|e_t\|_2 \leq (\rho^K)^t \|e_0\|_2 + \frac{2L}{K\gamma\Delta_{\min}} D\delta\lambda + O(\delta\lambda^2). \quad (\text{S2.138})$$

In particular if $\|e_0\|_2 = 0$,

$$\|e_t\|_2 \lesssim \frac{2L}{K} \frac{\sqrt{M} \|\partial_\lambda H(\lambda)\|_{\text{op}}}{\gamma^2 \Delta_{\min}^2} \delta\lambda. \quad (\text{S2.139})$$

Staying inside the PL region

To ensure that the iterates never leave the PL region, it suffices that the steady-state error remains below $r_{\text{PL}}/2$:

$$\frac{2L}{t\gamma\Delta_{\min}} D\delta\lambda = \frac{2L}{K} \frac{\sqrt{M} \|\partial_\lambda H(\lambda)\|_{\text{op}}}{\gamma^2 \Delta_{\min}^2} \delta\lambda \leq \frac{r_{\text{PL}}}{2} = \frac{\gamma\Delta_{\min}}{2L_H}. \quad (\text{S2.140})$$

Equivalently, a sufficient discretization condition is

$$\delta\lambda \leq \frac{t\gamma^2\Delta_{\min}^2}{4L_H L} \frac{1}{D} = \mathcal{O}\left(\frac{t\gamma^3\Delta_{\min}^3}{L_H L \sqrt{M} \|\partial_\lambda H\|_{\text{op}}}\right). \quad (\text{S2.141})$$

Under this condition, the warm-start iterations remain inside the PL region for all k , and the tracking error is uniformly bounded by Eq. S2.139.

Complexity

Each adiabatic step requires K gradient evaluations. The number of adiabatic steps is $T = 1/\delta\lambda$. Hence, the total number of gradient evaluations satisfies

$$N_{\text{updates}} = KT = \frac{K}{\delta\lambda} = \mathcal{O}\left(\frac{L_H L \sqrt{M} \|\partial_\lambda H\|_{\text{op}}}{\gamma^3 \Delta_{\min}^3}\right). \quad (\text{S2.142})$$

This yields the same asymptotic scaling as the analysis in Section S2.2.

Explicit complexity for Pauli-generated ansätze

Using the transient-error analysis framework, we evaluate the total gradient-update complexity N_{updates} by substituting the physical bounds derived in Section S1.1 for a variational ansatz composed of M Pauli-rotations. The total complexity is governed by the requirement that the steady-state tracking error remains within the Polyak–Łojasiewicz (PL) region, leading to the condition

$$N_{\text{updates}} \leq 384 \frac{M^3 \|H\|_{\text{op}}^2 \|H_f - H_i\|_{\text{op}}}{\gamma^3 \Delta_{\min}^3}.$$

(S2.143)

S3. PROOF OF THEOREM 1: CONTINUOUS-TIME ADIABATIC FORMULATION AND SCALING

The proof of Theorem 1 of the main text in the previous Section S2 does not offer a clear picture of why we get an extra $1/\Delta_{\min}$ factor on the number of gradient steps N_{updates} in comparison to the expected $1/\Delta_{\min}^2$ adiabatic scaling of the time complexity. In this section, we provide an alternative proof of the theorem using the time-dependent variational principle (TDVP). We demonstrate that, in the continuous-time formulation, the same scaling, $1/\Delta_{\min}^2$, is obtained. The extra $1/\Delta_{\min}$ factor comes from a *stability requirement* of discrete numerical integration methods. This stability factor is required for both explicit and more stable implicit solvers.

In the following, we first discuss the basics of the TDVP, then derive the continuous imaginary-time TDVP flow equations, and finally examine the numerical integration of the flow.

S3.1. Variational manifold and geometric structures

We consider a smooth variational manifold $\mathcal{M} \subset \mathbb{P}(\mathcal{H})$ embedded in projective Hilbert space, parametrized by real coordinates $\boldsymbol{\theta} = (\theta_\mu)_{\mu=1}^d$, with associated normalized quantum states $|\psi(\boldsymbol{\theta})\rangle \in \mathcal{H}$. The geometry of \mathcal{M} is inherited from the Fubini–Study metric. Define tangent vectors [2]

$$|\partial_\mu \psi\rangle = \frac{\partial}{\partial \theta_\mu} |\psi(\boldsymbol{\theta})\rangle, \quad \langle \psi | \psi \rangle = 1. \quad (\text{S3.144})$$

The quantum geometric tensor

$$Q_{\mu\nu} = \langle \partial_\mu \psi | \partial_\nu \psi \rangle - \langle \partial_\mu \psi | \psi \rangle \langle \psi | \partial_\nu \psi \rangle \quad (\text{S3.145})$$

induces a metric and a symplectic form:

$$g_{\mu\nu} = \text{Re } Q_{\mu\nu}, \quad \omega_{\mu\nu} = 2 \text{ Im } Q_{\mu\nu}. \quad (\text{S3.146})$$

On a Kähler manifold, these satisfy

$$\omega_{\mu\nu} = -g_{\mu\sigma} J^\sigma{}_\nu \quad (\text{S3.147})$$

with $J^\sigma{}_\nu$ the complex structure. Denote by

$$G^{\mu\nu}(\boldsymbol{\theta}) = [\mathbf{g}^{-1}]_{\mu\nu}(\boldsymbol{\theta}) \quad (\text{S3.148})$$

the inverse metric.

S3.2. Energy functional and TDVP flow

We again assume the setup defined in Section S1: the Hamiltonian depends smoothly on a dimensionless adiabatic parameter $\lambda \in [0, 1]$:

$$H(\lambda) = (1 - \lambda)H_i + \lambda H_f. \quad (\text{S3.149})$$

We again use the Assumptions 1-3 and define the energy functional on \mathcal{M} by

$$E(\boldsymbol{\theta}, \lambda) = \langle \psi(\boldsymbol{\theta}) | H(\lambda) | \psi(\boldsymbol{\theta}) \rangle. \quad (\text{S3.150})$$

Physical time is $\tau \in [0, T]$, with linear schedule

$$\lambda(\tau) = \frac{\tau}{T}. \quad (\text{S3.151})$$

The imaginary-time TDVP evolution is [2]

$$\frac{d\theta_\mu}{d\tau} = -G^{\mu\nu}(\boldsymbol{\theta}) \partial_\nu E(\boldsymbol{\theta}, \lambda). \quad (\text{S3.152})$$

S3.3. Linearized TDVP dynamics

Let $\boldsymbol{\theta}(\tau)$ be a solution of the TDVP equation (S3.152), and let

$$\delta\theta_\mu(\tau) = \theta_\mu(\tau) - \theta_\mu^*(\lambda(\tau))$$

denote the deviation from an instantaneous variational minimum $\boldsymbol{\theta}^*(\lambda)$. Differentiating $\delta\theta_\mu$ with respect to τ gives

$$\frac{d}{d\tau} \delta\theta_\mu(\tau) = \frac{d\theta_\mu}{d\tau} - \frac{d}{d\tau} \theta_\mu^*(\lambda(\tau)) = -G^{\mu\nu}(\boldsymbol{\theta}) \partial_\nu E(\boldsymbol{\theta}, \lambda) - \frac{1}{T} \partial_\lambda \theta_\mu^*(\lambda), \quad (\text{S3.153})$$

where we used the TDVP flow (S3.152) and the linear schedule $\lambda(\tau) = \tau/T$. By Taylor's remainder theorem for multivariate functions, we have

$$\partial_\nu E(\boldsymbol{\theta}^* + \delta\boldsymbol{\theta}, \lambda) = \partial_\nu E(\boldsymbol{\theta}^*, \lambda) + \mathcal{H}_{\sigma\nu}(\lambda) \delta\boldsymbol{\theta}^\sigma + R_\nu(\delta\boldsymbol{\theta}, \lambda), \quad (\text{S3.154})$$

where the Hessian at the minimum is

$$\mathcal{H}_{\mu\nu}(\lambda) = \partial_\mu \partial_\nu E(\boldsymbol{\theta}^*(\lambda), \lambda),$$

and the remainder R_ν satisfies the quadratic bound

$$\|R(\delta\boldsymbol{\theta}, \lambda)\|_2 \leq \frac{1}{2} L_E \|\delta\boldsymbol{\theta}\|_2^2, \quad L_E = \sup_{\boldsymbol{\theta} \in B(\boldsymbol{\theta}^*, r)} \|\nabla_{\boldsymbol{\theta}}^3 E(\boldsymbol{\theta}, \lambda)\|_{\text{op}}, \quad (\text{S3.155})$$

for $\|\delta\boldsymbol{\theta}\|_2$ sufficiently small. Since $\boldsymbol{\theta}^*(\lambda)$ is a minimizer, $\partial_\nu E(\boldsymbol{\theta}^*, \lambda) = 0$, so

$$\partial_\nu E(\boldsymbol{\theta}, \lambda) = \mathcal{H}_{\sigma\nu}(\lambda) \delta\boldsymbol{\theta}^\sigma + R_\nu(\delta\boldsymbol{\theta}, \lambda). \quad (\text{S3.156})$$

Similarly, for the metric inverse $G^{\mu\nu}(\boldsymbol{\theta})$, we have

$$G^{\mu\nu}(\boldsymbol{\theta}) = G^{\mu\nu}(\boldsymbol{\theta}^*) + \Delta G^{\mu\nu}(\delta\boldsymbol{\theta}), \quad \|\Delta\mathbf{G}(\delta\boldsymbol{\theta})\|_{\text{op}} \leq L_G \|\delta\boldsymbol{\theta}\|_2, \quad (\text{S3.157})$$

with L_G the Lipschitz constant of the metric. Substituting the expansions into the TDVP equation, we obtain

$$\frac{d}{d\tau} \delta\theta_\mu = -\left(G^{\mu\nu}(\boldsymbol{\theta}^*) + \Delta G^{\mu\nu}(\delta\boldsymbol{\theta})\right) \left(\mathcal{H}_{\sigma\nu} \delta\theta^\sigma + R_\nu(\delta\boldsymbol{\theta}, \lambda)\right) - \frac{1}{T} \partial_\lambda \theta_\mu^*(\lambda) \quad (\text{S3.158})$$

$$= K^\mu_\sigma(\lambda) \delta\theta^\sigma - \frac{1}{T} \partial_\lambda \theta_\mu^*(\lambda) + \underbrace{-\Delta G^{\mu\nu} \mathcal{H}_{\sigma\nu} \delta\theta^\sigma - (G^{\mu\nu} + \Delta G^{\mu\nu}) R_\nu}_{R^\mu(\delta\boldsymbol{\theta}, \lambda)}, \quad (\text{S3.159})$$

where we defined the linearized TDVP generator

$$K^\mu_\sigma(\lambda) = -G^{\mu\nu}(\boldsymbol{\theta}^*(\lambda)) \mathcal{H}_{\nu\sigma}(\lambda), \quad (\text{S3.160})$$

and collected all higher-order nonlinear terms in

$$R^\mu(\delta\boldsymbol{\theta}, \lambda) = -\Delta G^{\mu\nu} \mathcal{H}_{\sigma\nu} \delta\theta^\sigma - (G^{\mu\nu} + \Delta G^{\mu\nu}) R_\nu(\delta\boldsymbol{\theta}, \lambda). \quad (\text{S3.161})$$

By the submultiplicativity of the operator norm,

$$\|R(\delta\boldsymbol{\theta}, \lambda)\|_2 \leq C_{\text{nl}} \|\delta\boldsymbol{\theta}\|_2^2, \quad C_{\text{nl}} = \frac{1}{2} L_E \|\mathbf{G}\|_{\text{op}} + L_G \|\mathcal{H}\|_{\text{op}}. \quad (\text{S3.162})$$

The deviation from the instantaneous minimizer thus satisfies

$$\boxed{\frac{d}{d\tau} \delta\boldsymbol{\theta}(\tau) = \mathbf{K}(\lambda) \delta\boldsymbol{\theta}(\tau) - \frac{1}{T} \partial_\lambda \theta^*(\lambda) + R(\delta\boldsymbol{\theta}, \lambda), \quad \|R(\delta\boldsymbol{\theta}, \lambda)\|_2 \leq C_{\text{nl}} \|\delta\boldsymbol{\theta}\|_2^2.} \quad (\text{S3.163})$$

S3.4. Explicit evaluation of the nonlinear constant C_{nl}

For the final scaling, we need an explicit bound for the nonlinear remainder constant C_{nl} appearing in Eq. S3.162. Throughout, we consider the Pauli-rotation ansatz $|\psi(\boldsymbol{\theta})\rangle = \prod_{j=0}^{M-1} e^{-iP_j\theta_j} |0\rangle$ with $\|P_j\|_{\text{op}} = 1$.

We have to upper bound the following terms

$$C_{\text{nl}} = \frac{1}{2} L_E \|\mathbf{G}\|_{\text{op}} + L_G \|\mathcal{H}\|_{\text{op}},$$

where

$$L_E = \sup_{\boldsymbol{\theta} \in B(\boldsymbol{\theta}^*, r)} \|\nabla_{\boldsymbol{\theta}}^3 E(\boldsymbol{\theta}, \lambda)\|_{\text{op}}, \quad (\text{S3.164})$$

$$L_G : \|G(\boldsymbol{\theta}) - G(\boldsymbol{\theta}^*)\|_{\text{op}} \leq L_G \|\boldsymbol{\theta} - \boldsymbol{\theta}^*\|_2. \quad (\text{S3.165})$$

Third-derivative bound L_E

From the commutator representation of third derivatives derived in Section S1,

$$\partial_m \partial_k \partial_\ell E(\boldsymbol{\theta}) = \langle \psi | [[\tilde{P}_m, \tilde{P}_k], [\tilde{P}_\ell, H]] | \psi \rangle + \text{permutations}, \quad (\text{S3.166})$$

and using $\|\tilde{P}_j\|_{\text{op}} = 1$ together with $\|[X, Y]\|_{\text{op}} \leq 2\|X\|_{\text{op}}\|Y\|_{\text{op}}$, each nested commutator term obeys

$$|\partial_m \partial_k \partial_\ell E| \leq 8\|H\|_{\text{op}}. \quad (\text{S3.167})$$

The operator norm of the third-derivative tensor is defined as

$$\|\nabla_{\boldsymbol{\theta}}^3 E\|_{\text{op}} = \sup_{\|u\|_2 = \|v\|_2 = \|w\|_2 = 1} \left| \sum_{m, k, \ell} u_m v_k w_\ell \partial_m \partial_k \partial_\ell E \right|. \quad (\text{S3.168})$$

Grouping the sum by the first index and using $\|u\|_1 \leq \sqrt{M}\|u\|_2$ gives

$$\|\nabla_{\boldsymbol{\theta}}^3 E\|_{\text{op}} \leq \sqrt{M} \max_m \|\nabla_m^3 E\|_{\text{op}}. \quad (\text{S3.169})$$

With the bound $\|\nabla_m^3 E\|_{\text{op}} \leq 24\|H\|_{\text{op}}M$ derived in Eq. S2.58 we obtain the explicit constant

$$\boxed{L_E \leq 24 \|H\|_{\text{op}} M^{3/2}.} \quad (\text{S3.170})$$

Lipschitz constant of the inverse metric

To bound L_G in Eq. (S3.160) we control the Jacobian of $G = g^{-1}$. For any θ, θ' in a neighborhood B ,

$$\|G(\theta') - G(\theta)\|_{\text{op}} \leq \sup_{\xi \in B} \left\| \sum_{k=1}^M v_k \partial_k G(\xi) \right\|_{\text{op}} \|\theta' - \theta\|_2,$$

and using $\|v\|_1 \leq \sqrt{M}\|v\|_2$ we obtain

$$L_G \leq \sqrt{M} \sup_{\theta \in B} \max_k \|\partial_k G(\theta)\|_{\text{op}}.$$

Differentiating $G(\theta) = g(\theta)^{-1}$ yields $\partial_k G(\theta) = -G(\theta)(\partial_k g(\theta))G(\theta)$ and hence

$$\|\partial_k G(\theta)\|_{\text{op}} \leq \|G(\theta)\|_{\text{op}}^2 \|\partial_k g(\theta)\|_{\text{op}}.$$

For the Pauli-rotation ansatz with $\|\tilde{P}_j\|_{\text{op}} = 1$ the metric can be written as a covariance of \tilde{P}_μ , and the identity $\partial_k \langle A \rangle = i \langle [\tilde{P}_k, A] \rangle$ implies

$$|\partial_k g_{\mu\nu}| \leq \|[\tilde{P}_k, \tilde{P}_\mu \tilde{P}_\nu]\|_{\text{op}} + \|[\tilde{P}_k, \tilde{P}_\mu]\|_{\text{op}} |\langle \tilde{P}_\nu \rangle| + |\langle \tilde{P}_\mu \rangle| \|[\tilde{P}_k, \tilde{P}_\nu]\|_{\text{op}} \leq 6,$$

so $\|\partial_k g(\theta)\|_{\text{op}} \leq 6M$. Assuming $g(\theta) \succeq (\gamma/2)I$ on B , we have $\|G(\theta)\|_{\text{op}} \leq 2/\gamma$ and therefore

$$\|\partial_k G(\theta)\|_{\text{op}} \leq (2/\gamma)^2 (6M) = 24M/\gamma^2, \quad L_G \leq \sqrt{M} 24M/\gamma^2 = 24M^{3/2}/\gamma^2.$$

Final bound on C_{nl}

Using Lemma 2, the Hessian of the variational energy obeys $\|\mathcal{H}(\theta, \lambda)\|_{\text{op}} = \|\nabla_\theta^2 E(\theta, \lambda)\|_{\text{op}} \leq 4\|H(\lambda)\|_{\text{op}} M$. Therefore

$$\begin{aligned} C_{\text{nl}} &\leq \frac{1}{2} \left(24\|H\|_{\text{op}} M^{3/2} \right) \frac{1}{\gamma} + \left(\frac{8M^{3/2}}{\gamma^2} \right) \|\mathcal{H}\|_{\text{op}} \\ &\leq \frac{12}{\gamma} \|H\|_{\text{op}} M^{3/2} + \frac{32}{\gamma^2} \|H\|_{\text{op}} M^{5/2} \approx \frac{32}{\gamma^2} \|H\|_{\text{op}} M^{5/2}. \end{aligned} \quad (\text{S3.171})$$

S3.5. Imaginary-time ground state following

The following theorem is an imaginary time version of the theorem proven in [3].

Theorem 1 (Imaginary-time ground state variational adiabatic theorem). *Let $\boldsymbol{\theta}(\tau)$ satisfy (S3.152). Then*

$$\|\delta\boldsymbol{\theta}(\tau)\|_2 \leq \frac{D}{T\Delta_{\min}} (1 - e^{-\Delta_{\min}\tau}), \quad \forall \tau \in [0, T]. \quad (\text{S3.172})$$

Proof. Let

$$\delta\boldsymbol{\theta}(\tau) = \boldsymbol{\theta}(\tau) - \boldsymbol{\theta}^*(\lambda(\tau)), \quad u(\tau) = \|\delta\boldsymbol{\theta}(\tau)\|_2.$$

From Eq. S3.163, the deviation satisfies

$$\dot{\delta\boldsymbol{\theta}} = \mathbf{K}(\lambda) \delta\boldsymbol{\theta} - \frac{1}{T} \partial_\lambda \boldsymbol{\theta}^*(\lambda) + \mathcal{R}(\delta\boldsymbol{\theta}, \lambda),$$

with $\|\mathcal{R}(\delta\boldsymbol{\theta}, \lambda)\|_2 \leq C_{\text{nl}} \|\delta\boldsymbol{\theta}\|_2^2$. For $u(\tau) > 0$, differentiating the norm yields

$$\frac{d}{d\tau} u = \frac{\langle \delta\boldsymbol{\theta}, \dot{\delta\boldsymbol{\theta}} \rangle}{\|\delta\boldsymbol{\theta}\|_2}.$$

Substituting the evolution equation gives

$$\frac{d}{d\tau}u = \frac{\langle \delta\boldsymbol{\theta}, \mathbf{K}(\lambda)\delta\boldsymbol{\theta} \rangle}{\|\delta\boldsymbol{\theta}\|_2} - \frac{1}{T} \frac{\langle \delta\boldsymbol{\theta}, \partial_\lambda \boldsymbol{\theta}^* \rangle}{\|\delta\boldsymbol{\theta}\|_2} + \frac{\langle \delta\boldsymbol{\theta}, \mathcal{R}(\delta\boldsymbol{\theta}, \lambda) \rangle}{\|\delta\boldsymbol{\theta}\|_2}. \quad (\text{S3.173})$$

By Assumption 3, the linearized TDVP generator $\mathbf{K}(\lambda) = -\mathbf{G}(\boldsymbol{\theta}^*)\mathcal{H}(\lambda)$ is strictly dissipative on the subspace orthogonal to gauge directions, i.e.,

$$\langle x, \mathbf{K}(\lambda)x \rangle \leq -\Delta_{\min} \|x\|_2^2 \quad \forall x \perp \text{gauge}.$$

Since $\delta\boldsymbol{\theta}$ is defined modulo gauge equivalence, this yields

$$\frac{\langle \delta\boldsymbol{\theta}, \mathbf{K}(\lambda)\delta\boldsymbol{\theta} \rangle}{\|\delta\boldsymbol{\theta}\|_2} \leq -\Delta_{\min} u.$$

Using Cauchy–Schwarz and the drift bound Lemma 6,

$$\frac{1}{T} \frac{|\langle \delta\boldsymbol{\theta}, \partial_\lambda \boldsymbol{\theta}^* \rangle|}{\|\delta\boldsymbol{\theta}\|_2} \leq \frac{1}{T} \|\partial_\lambda \boldsymbol{\theta}^*\|_2 \leq \frac{D}{T}.$$

Similarly, using the quadratic bound on the nonlinear remainder,

$$\frac{|\langle \delta\boldsymbol{\theta}, \mathcal{R}(\delta\boldsymbol{\theta}, \lambda) \rangle|}{\|\delta\boldsymbol{\theta}\|_2} \leq \|\mathcal{R}(\delta\boldsymbol{\theta}, \lambda)\|_2 \leq C_{\text{nl}} u^2.$$

Combining the above estimates in Eq. (S3.173), we obtain

$$\frac{d}{d\tau}u \leq -\Delta_{\min} u + \frac{D}{T} + C_{\text{nl}} u^2.$$

Since $u(0) = 0$ and the solution remains $O(1/T)$ for finite τ , the quadratic term is higher order in $1/T$ and can be discarded for an upper bound, yielding

$$\frac{d}{d\tau}u \leq -\Delta_{\min} u + \frac{D}{T}.$$

The next step provides a self-consistent justification of the approximation by dropping the quadratic term.

Solving this differential inequality with $u(0) = 0$ gives

$$u(\tau) \leq \frac{D}{T\Delta_{\min}} (1 - e^{-\Delta_{\min}\tau}), \quad \tau \in [0, T].$$

□

At this stage, we still have the optimal adiabatic complexity $1/\Delta_{\min}^2$, since $D = \mathcal{O}(1/\Delta_{\min})$. In the following section, we see that discrete updates introduce an additional $1/\Delta_{\min}$ due to stability, analogous to the condition that the optimised parameters should remain in the PL region.

S3.6. Numerical stability and gradient-update complexity

Discrete-time TDVP update

We discretize the imaginary-time TDVP flow

$$\frac{d\boldsymbol{\theta}}{d\tau} = -\mathbf{G}(\boldsymbol{\theta})\nabla_{\boldsymbol{\theta}}E(\boldsymbol{\theta}, \lambda), \quad (\text{S3.174})$$

with step size $\eta > 0$ and linear schedule $\lambda_n = n\eta/T$, $n = 0, 1, \dots, N_{\text{updates}} - 1$, $N_{\text{updates}} = T/\eta$:

$$\boldsymbol{\theta}_{n+1} = \boldsymbol{\theta}_n - \eta \mathbf{G}(\boldsymbol{\theta}_n) \nabla_{\boldsymbol{\theta}}E(\boldsymbol{\theta}_n, \lambda_n). \quad (\text{S3.175})$$

Let the deviation from the instantaneous minimizer be

$$\delta\boldsymbol{\theta}_n = \boldsymbol{\theta}_n - \boldsymbol{\theta}^*(\lambda_n), \quad (\text{S3.176})$$

where $\boldsymbol{\theta}^*(\lambda)$ is the exact variational ground state for each λ .

Linearization and nonlinear bounds

Expand the gradient and metric:

$$\nabla_{\boldsymbol{\theta}} E(\boldsymbol{\theta}_n, \lambda_n) = \mathcal{H}(\lambda_n) \delta \boldsymbol{\theta}_n + R_n, \quad \|R_n\|_2 \leq \frac{1}{2} L_E \|\delta \boldsymbol{\theta}_n\|_2^2, \quad (\text{S3.177})$$

$$\mathbf{G}(\boldsymbol{\theta}_n) = \mathbf{G}(\boldsymbol{\theta}^*(\lambda_n)) + \Delta \mathbf{G}_n, \quad \|\Delta \mathbf{G}_n\|_{\text{op}} \leq L_G \|\delta \boldsymbol{\theta}_n\|_2. \quad (\text{S3.178})$$

Then the discrete deviation satisfies

$$\delta \boldsymbol{\theta}_{n+1} = (I - \eta \mathbf{K}_n) \delta \boldsymbol{\theta}_n - (\boldsymbol{\theta}^*(\lambda_{n+1}) - \boldsymbol{\theta}^*(\lambda_n)) - \eta (\Delta \mathbf{G}_n \mathcal{H} \delta \boldsymbol{\theta}_n + (\mathbf{G} + \Delta \mathbf{G}_n) R_n). \quad (\text{S3.179})$$

Using the submultiplicativity of operator norms together with (S3.177)–(S3.178), we estimate

$$\|\Delta \mathbf{G}_n \mathcal{H}(\lambda_n) \delta \boldsymbol{\theta}_n\|_2 \leq \|\Delta \mathbf{G}_n\|_{\text{op}} \|\mathcal{H}\|_{\text{op}} \|\delta \boldsymbol{\theta}_n\|_2 \leq L_G \|\mathcal{H}\|_{\text{op}} \|\delta \boldsymbol{\theta}_n\|_2^2, \quad (\text{S3.180})$$

$$\|(\mathbf{G}(\boldsymbol{\theta}_n)) R_n\|_2 \leq \|\mathbf{G}(\boldsymbol{\theta}_n)\|_{\text{op}} \|R_n\|_2 \leq \|\mathbf{G}\|_{\text{op}} \frac{1}{2} L_E \|\delta \boldsymbol{\theta}_n\|_2^2, \quad (\text{S3.181})$$

Combining both contributions yields

$$\|\mathbf{G}(\boldsymbol{\theta}_n) \nabla_{\boldsymbol{\theta}} E(\boldsymbol{\theta}_n, \lambda_n) - \mathbf{g}(\boldsymbol{\theta}^*) \mathcal{H}(\lambda_n) \delta \boldsymbol{\theta}_n\|_2 \leq C_{\text{nl}} \|\delta \boldsymbol{\theta}_n\|_2^2, \quad (\text{S3.182})$$

where C_{nl} is the same as in the continuous case Eq. S3.162. Substituting (S3.5), (S3.182), and Lemma 6 into (S3.179) and applying the triangle inequality, we obtain

$$\boxed{\|\delta \boldsymbol{\theta}_{n+1}\|_2 \leq (1 - \eta \Delta_{\min}) \|\delta \boldsymbol{\theta}_n\|_2 + b + c \|\delta \boldsymbol{\theta}_n\|_2^2}, \quad (\text{S3.183})$$

where $c = \eta C_{\text{nl}}$.

Global discrete tracking bound

Theorem 2 (Uniform discrete tracking bound). *Let $\delta \boldsymbol{\theta}_n = \boldsymbol{\theta}_n - \boldsymbol{\theta}^*(\lambda_n)$ satisfy the discrete TDVP update with $\delta \boldsymbol{\theta}^* = 0$. Assume that the step size satisfies*

$$0 < \eta \leq \frac{1}{2 \|\mathcal{H}\|_{\text{op}}}, \quad (\text{S3.184})$$

and that the total evolution time T satisfies

$$T \geq \frac{4 C_{\text{nl}} D}{\Delta_{\min}^2}. \quad (\text{S3.185})$$

Define

$$A = \frac{2D}{T \Delta_{\min}}. \quad (\text{S3.186})$$

Then for all $n = 0, 1, \dots, N_{\text{updates}}$,

$$\|\delta \boldsymbol{\theta}_n\|_2 \leq A. \quad (\text{S3.187})$$

In particular, the iterates remain inside the locality radius where the perturbations in Eq. S3.177 and Eq. S3.178 remain valid.

Remark 1. Due to stability, the time T has to scale as $1/\Delta_{\min}^3$, whereas the error scales as $1/T \Delta_{\min}^2$.

Proof. Define

$$a_n = \|\delta \boldsymbol{\theta}_n\|_2.$$

By Eq. S3.183, the sequence $\{a_n\}_{n \geq 0}$ satisfies the deterministic recursion

$$a_{n+1} \leq (1 - \eta \Delta_{\min}) a_n + b + c a_n^2, \quad (\text{S3.188})$$

where

$$b = \eta \frac{D}{T}, \quad c = \eta C_{\text{nl}}.$$

We prove by induction that

$$a_n \leq A \quad \text{for all } n \geq 0,$$

with A defined in (S3.186). By assumption, $\delta\theta^* = 0$, hence

$$a_0 = 0 \leq A.$$

Assume $a_n \leq A$ for some $n \geq 0$. We show that $a_{n+1} \leq A$. Using (S3.188) and the induction hypothesis,

$$a_{n+1} \leq (1 - \eta \Delta_{\min}) A + b + cA^2. \quad (\text{S3.189})$$

Thus, it suffices to verify that

$$(1 - \eta \Delta_{\min}) A + b + cA^2 \leq A. \quad (\text{S3.190})$$

Rearranging (S3.190) gives the quadratic inequality

$$cA^2 - \eta \Delta_{\min} A + b \leq 0. \quad (\text{S3.191})$$

Consider the quadratic polynomial

$$p(a) = ca^2 - \eta \Delta_{\min} a + b.$$

Assume the discriminant is nonnegative,

$$\text{Disc} = \eta^2 \Delta_{\min}^2 - 4bc \geq 0. \quad (\text{S3.192})$$

Then p has two real roots

$$A_{\pm} = \frac{\eta \Delta_{\min} \pm \sqrt{\text{Disc}}}{2c}, \quad 0 < A_- \leq A_+.$$

Moreover, on $[0, A_-]$ we have $1 - \eta \Delta_{\min} + 2ca \geq 0$. Hence, for any $a \in [0, A_-]$,

$$(1 - \eta \Delta_{\min}) a + b + ca^2 < A_-.$$

Since $a_0 = 0 \in [0, A_-]$, we obtain by induction that

$$a_n \leq A_- \quad \text{for all } n = 0, 1, \dots, N_{\text{updates}}.$$

Thus, the *guaranteed tracking region* can be chosen as the smaller root

$$A = A_- = \frac{\eta \Delta_{\min} - \sqrt{\eta^2 \Delta_{\min}^2 - 4bc}}{2c}. \quad (\text{S3.193})$$

The smaller root can be rewritten as

$$A_- = \frac{\eta \Delta_{\min} - \sqrt{\eta^2 \Delta_{\min}^2 - 4bc}}{2c} = \frac{2b}{\eta \Delta_{\min} + \sqrt{\eta^2 \Delta_{\min}^2 - 4bc}},$$

where the second equality follows by multiplying the numerator and denominator by $\eta \Delta_{\min} + \sqrt{\eta^2 \Delta_{\min}^2 - 4bc}$. Since $\sqrt{\eta^2 \Delta_{\min}^2 - 4bc} \geq 0$, we obtain the upper bound

$$A_- \leq \frac{2b}{\eta \Delta_{\min}}.$$

Using $b = \eta D/T$, this yields the sufficient choice

$$A \leq \frac{2D}{T\Delta_{\min}},$$

which coincides with (S3.186). The discriminant condition (S3.192) becomes

$$\eta^2 \Delta_{\min}^2 \geq 4bc \iff \Delta_{\min}^2 \geq 4C_{\text{nl}} \frac{D}{T},$$

i.e.

$$T \geq \frac{4C_{\text{nl}}D}{\Delta_{\min}^2},$$

which is exactly the hypothesis (S3.185). By induction,

$$a_n = \|\delta\theta_n\|_2 \leq A \quad \text{for all } n = 0, 1, \dots, N_{\text{updates}}.$$

Finally, using (S3.185)

$$A = \frac{2D}{T\Delta_{\min}} \leq \frac{\Delta_{\min}}{2C_{\text{nl}}}$$

Hence, all iterates remain inside the region where Eq. S3.183 applies. \square

Gradient-update complexity

To achieve tracking error $\|\delta\theta\|_2 \leq \varepsilon$, one must satisfy

$$T \geq \max \left\{ \frac{4C_{\text{nl}}D}{\Delta_{\min}^2}, \frac{2D}{\varepsilon\Delta_{\min}} \right\}, \quad (\text{S3.194})$$

with step size $\eta = 1/(2\|H\|_{\text{op}})$. Therefore, the number of gradient updates is

$$N_{\text{updates}} = \frac{T}{\eta} \geq 4\|H\|_{\text{op}} \frac{D}{\Delta_{\min}} \max \left\{ \frac{C_{\text{nl}}}{\Delta_{\min}}, \frac{1}{\varepsilon} \right\}. \quad (\text{S3.195})$$

Using $D = \frac{\sqrt{M}\|\partial_{\lambda}H\|_{\text{op}}}{\gamma\Delta_{\min}}$ and the dominant contribution $C_{\text{nl}} \simeq \frac{32}{\gamma^2}\|H\|_{\text{op}}M^{5/2}$, Eq. S3.171 yields the approximate scaling

$$N_{\text{update}} \simeq 128 \frac{M^3\|H\|_{\text{op}}^2\|H_f - H_i\|_{\text{op}}}{\gamma^3\Delta_{\min}^3}, \quad (\text{S3.196})$$

up to subleading terms in M and universal numerical constants.

S3.7. Comparison of PL and TDVP scalings.

The three analyses presented above provide complementary perspectives on the same tracking dynamics. Both PL constructions yield the same overall update complexity $N_{\text{updates}} \propto \Delta_{\min}^{-3}$, but distribute the cost differently: PL **option 1** employs comparatively large adiabatic steps $\delta\lambda \propto \Delta_{\min}^2$ together with many optimization steps per slice $K \propto \Delta_{\min}^{-1}$, whereas PL **option 2** keeps $K = \mathcal{O}(1)$ and compensates by refining the discretization to $\delta\lambda \propto \Delta_{\min}^3$. The TDVP derivation instead starts from a continuous-time imaginary-time flow, which exhibits the expected adiabatic scaling $T \propto \Delta_{\min}^{-2}$. For explicit discretizations, an additional factor Δ_{\min}^{-1} appears due to the stability constraint on the update size, reflecting the stiffness of the gradient flow near small gaps.

Implicit (proximal-point) discretizations provide a complementary interpretation. While such schemes remove the explicit stability restriction on the step size and allow larger adiabatic increments [4], each proximal update corresponds to solving a strongly convex subproblem whose contraction rate scales as $\mu \sim \gamma\Delta_{\min}$. Consequently, the additional Δ_{\min}^{-1} factor reappears through the inner optimization effort, making proximal TDVP closely analogous to PL **option 1** [5].

From a physical perspective, this behaviour reflects the intrinsic adiabatic curvature of the variational manifold: as the spectral gap narrows, the local contraction rate governing relaxation towards the instantaneous ground-state branch decreases proportionally to Δ_{\min} , so that any local first-order tracking scheme—explicit or implicit—requires $\mathcal{O}(\Delta_{\min}^{-1})$ relaxation steps per adiabatic time scale. Thus, the extra gap dependence is not merely a numerical artefact of explicit integration, but a manifestation of the geometric slowdown near small gaps, and all viewpoints consistently lead to the same asymptotic update scaling while illuminating different allocations of computational effort.

S4. ABSENCE OF BARREN PLATEAUS

In this section, we present a proof of the absence of barren plateaus, i.e., gradients that decrease exponentially with the system size, when we are exploring the energy landscape close to a minimum. The proof can be explained in the following way: we write the energy cost function in Taylor form around the minimum $\boldsymbol{\theta}^*$, and choose a small-enough radius r such that we can approximate the energy as a quadratic form up to error ϵ_Q . In this approximation, we show that the variance of the loss function does not decay exponentially with system size. We stress that we are proving a stronger condition than the presence of gradients: we show the region where the energy is approximately quadratic.

Theorem 3 (Non-vanishing variance of the energy close to the minimum). *Let $|\psi(\boldsymbol{\theta})\rangle$ be the variational ansatz with M parameters, and let $\boldsymbol{\theta}^*$ be the minimum of the energy function $E(\boldsymbol{\theta}) = \langle\psi(\boldsymbol{\theta})|H|\psi(\boldsymbol{\theta})\rangle$. Suppose the perturbations $\delta\boldsymbol{\theta}$ are independently identically distributed variables drawn from the normal distribution:*

$$\delta\theta_j \sim N\left(0, \frac{\epsilon_Q}{12\|H\|_{\text{op}}M^{3/2}}\right). \quad (\text{S4.197})$$

Then, the energy variance is polynomial in the number of parameters M , i.e.:

$$\text{Var}_{\delta\boldsymbol{\theta}}[E(\boldsymbol{\theta}^* + \delta\boldsymbol{\theta})] \geq \frac{\Delta_{\min}^6 \epsilon_Q^4}{12^4 \|H\|_{\text{op}}^4 M^7} \left(\sum_k 1 - \left| \langle \hat{0} | \tilde{P}_k | \hat{0} \rangle \right|^2 \right)^2. \quad (\text{S4.198})$$

with $\epsilon_Q \in (0, 1)$.

Proof. We start by determining the radius for which $E(\boldsymbol{\theta}^* + \delta\boldsymbol{\theta})$ can be approximated as a quadratic form, i.e.:

$$E(\boldsymbol{\theta}^* + \delta\boldsymbol{\theta}) = E(\boldsymbol{\theta}^*) + \frac{1}{2}\delta\boldsymbol{\theta}^T \mathcal{H}(\boldsymbol{\theta}^*)\delta\boldsymbol{\theta} + \frac{1}{6}\sum_{ijk} T_{ijk}(\boldsymbol{\theta})\delta\theta^3 \approx E(\boldsymbol{\theta}^*) + \frac{1}{2}\delta\boldsymbol{\theta}^T \mathcal{H}(\boldsymbol{\theta}^*)\delta\boldsymbol{\theta}, \quad (\text{S4.199})$$

which leads to the condition on the perturbation $\delta\boldsymbol{\theta}$:

$$\delta\boldsymbol{\theta} \leq 3\epsilon_Q \frac{\|\mathcal{H}(\boldsymbol{\theta}^*)\|_{\text{op}}}{\max_{\boldsymbol{\theta} \in (\boldsymbol{\theta}^* + \delta\boldsymbol{\theta})} \|T(\boldsymbol{\theta})\|_{\text{op}}}. \quad (\text{S4.200})$$

To have a rigorous bound, we first lower-bound the numerator and then upper-bound the denominator. For the numerator, we use Lemma 4 to bound $\|\mathcal{H}\|_{\text{op}}$:

$$\|\mathcal{H}\|_{\text{op}} \geq 2\gamma\Delta_{\min}, \quad (\text{S4.201})$$

and for the denominator we recall Eq. (S3.170):

$$\|T\|_{\text{op}} \leq 24M^{3/2}\|H\|_{\text{op}}. \quad (\text{S4.202})$$

The radius $\delta\theta_Q$ where we can approximate the energy as a quadratic form reads:

$$\delta\boldsymbol{\theta} \leq \delta\theta_Q = \epsilon_Q \frac{\gamma\Delta_{\min}}{12M^{3/2}\|H\|_{\text{op}}}. \quad (\text{S4.203})$$

For $\delta\boldsymbol{\theta} \leq \delta\theta_Q$, we can write the energy as:

$$E(\boldsymbol{\theta}^* + \delta\boldsymbol{\theta}) \approx E(\boldsymbol{\theta}^*) + \frac{1}{2}\delta\boldsymbol{\theta}^T \mathcal{H}(\boldsymbol{\theta}^*)\delta\boldsymbol{\theta}, \quad (\text{S4.204})$$

and the variance of the energy becomes:

$$\text{Var}_{\delta\theta} [E(\boldsymbol{\theta}^* + \delta\theta)] \approx \frac{1}{2} \text{Var}_{\delta\theta} [\delta\theta^T \mathcal{H}(\boldsymbol{\theta}^*) \delta\theta]. \quad (\text{S4.205})$$

When each i.i.d. random variable $\delta\theta$ is drawn from a normal distribution of mean $\mu = 0$ and standard deviation $\sigma = \delta\theta_Q$ the variance of the quadratic form is well known [6]:

$$\text{Var}_{\delta\theta} [\delta\theta^T \mathcal{H}(\boldsymbol{\theta}^*) \delta\theta] = \frac{\delta\theta_Q^4}{2} \|\mathcal{H}\|_F^2 \geq \frac{\delta\theta_Q^4}{2M} \text{Tr}\{\mathcal{H}\}^2. \quad (\text{S4.206})$$

We focus on the diagonal element of the Hessian in spectral form, where $|\hat{n}\rangle$ is the n -th eigenvector of the Hamiltonian H :

$$\mathcal{H}_{kk}(\boldsymbol{\theta}^*) = 2 \sum_{n \geq 1} (E_i - E_0) \left| \langle \hat{0} | \tilde{P}_k | \hat{n} \rangle \right|^2 \geq 2(E_1 - E_0) \sum_{n \geq 1} \left| \langle \hat{0} | \tilde{P}_k | \hat{n} \rangle \right|^2 \quad (\text{S4.207})$$

$$= 2\Delta_{10} \sum_{n \geq 1} \langle \hat{0} | \tilde{P}_k | \hat{n} \rangle \langle \hat{n} | \tilde{P}_k | \hat{0} \rangle = 2\Delta_{10} \left(\sum_{n \geq 0} \langle \hat{0} | \tilde{P}_k | \hat{n} \rangle \langle \hat{n} | \tilde{P}_k | \hat{0} \rangle - \left| \langle \hat{0} | \tilde{P}_k | \hat{0} \rangle \right|^2 \right) \quad (\text{S4.208})$$

$$= 2\Delta_{10} \left(\langle \hat{0} | \tilde{P}_k^2 | \hat{0} \rangle - \left| \langle \hat{0} | \tilde{P}_k | \hat{0} \rangle \right|^2 \right) = 2\Delta_{10} \left(1 - \left| \langle \hat{0} | \tilde{P}_k | \hat{0} \rangle \right|^2 \right) \geq 2\Delta_{\min} \left(1 - \left| \langle \hat{0} | \tilde{P}_k | \hat{0} \rangle \right|^2 \right), \quad (\text{S4.209})$$

where Δ_{\min} is the minimum gap across the adiabatic path. Thus, we obtain:

$$\frac{1}{2} \text{Var}_{\delta\theta} [\delta\theta^T \mathcal{H}(\boldsymbol{\theta}^*) \delta_{\min} \theta] \geq \frac{\delta\theta_Q^4}{4M} 4\Delta^2 \left(\sum_k 1 - \left| \langle \hat{0} | \tilde{P}_k | \hat{0} \rangle \right|^2 \right)^2 = \frac{\Delta_{\min}^6}{12^4 \|H\|_{\text{op}}^4 M^7} \left(\sum_k 1 - \left| \langle \hat{0} | \tilde{P}_k | \hat{0} \rangle \right|^2 \right)^2. \quad (\text{S4.210})$$

Note that in the best case scenario, when $\left| \langle \hat{0} | \tilde{P}_k | \hat{0} \rangle \right| \approx$ we can obtain:

$$\text{Var}_{\delta\theta} [E(\boldsymbol{\theta}^* + \delta\theta)] \approx \frac{\epsilon_Q^4 \Delta_{\min}^6}{12^4 \|H\|_{\text{op}}^4 M^5} \quad (\text{S4.211})$$

□

S5. PROOF OF THEOREM 2: STANDARD-DEVIATION-BASED VERIFICATION

In this section, we introduce a *verification layer* which certifies, at each adiabatic step, that the variational state lies on the correct (ground-state) spectral branch. The verification procedure is entirely based on measurements of the energy standard deviation and is logically independent of the optimization method used to update the variational parameters. Throughout this section, the standard deviation is used solely as a *diagnostic observable*. It does not drive the optimization but serves to certify eigen-branch identity and, once the branch is identified, to quantify the overlap with the corresponding eigenstate.

S5.1. Setup, assumptions, and proof roadmap

To make the presentation easier, we extend our setup and assumptions from Section S1. We define the spectral decomposition

$$H(\lambda) = \sum_{j \geq 0} E_j(\lambda) \Pi_j(\lambda), \quad E_0(\lambda) < E_1(\lambda) \leq E_2(\lambda) \leq \dots,$$

where $\Pi_j(\lambda)$ denotes a projector to j -th eigenstate. For any normalized state $|\psi\rangle$ and Hermitian operator A , we define

$$\sigma_\psi(A) = \sqrt{\langle \psi | A^2 | \psi \rangle - \langle \psi | A | \psi \rangle^2}, \quad (\text{S5.212})$$

$$E_\psi(\lambda) = \langle \psi | H(\lambda) | \psi \rangle, \quad \text{and} \quad \sigma_\psi(\lambda) = \sigma_\psi(H(\lambda)). \quad (\text{S5.213})$$

In addition, we introduce a new assumption.

Assumption 4 (Uniform gap to the tracked branch). *Let j_* denote the eigen-branch. Assume there exists $\Delta_{\min}^{j_*} > 0$ such that, for all $\lambda \in [0, 1]$,*

$$\min_{j \neq j_*} |E_j(\lambda) - E_{j_*}(\lambda)| \geq \Delta_{\min}^{j_*}. \quad (\text{S5.214})$$

For the main theorem, we use $j_* = 0$ (which reduces Assumption 4 to Assumption 1), but we state some lemmas more generally.

Proof roadmap: The goal of this section is to turn *measured energy standard deviation* into a *runtime verification* that the algorithm remains on the intended eigen-branch (in particular, the ground-state branch) throughout the adiabatic evolution, and to quantify the resulting fidelity. The proof of **Theorem 2** in the main text is obtained in several steps:

1. **Eigen-branch identification from standard deviation.** First, we show that, for any state $|\psi\rangle$ at a fixed λ , the mean energy $E_\psi(\lambda)$ must lie within one standard deviation of *some* eigenvalue $E_j(\lambda)$. Moreover, if the measured standard deviation is smaller than half the uniform branch gap, then this index is *unique*. This is Lemma 8.
2. **From identification to fidelity.** Once the relevant branch j_* is uniquely identified, we convert the same standard deviation value into a quantitative lower bound on the overlap $\langle \psi | \Pi_{j_*}(\lambda) | \psi \rangle$. This is Lemma 9 and its specialization to the ground state in Corollary 1. In our final theorem, we use $j_* = 0$.
3. **Warm-start verification for linear schedules.** We then analyze the canonical warm-start state $|0(\lambda)\rangle$ when the schedule advances to $\lambda^+ = \lambda + \delta\lambda$. For a linear interpolation $H(\lambda)$, the energy standard deviation of the warm start with respect to the *new* Hamiltonian is *exactly quadratic* in $\delta\lambda$, yielding an explicit step-size condition that guarantees $\sigma_{0(\lambda)}(H(\lambda^+)) < \Delta_{\min}/2$. This is Lemma 10 and the subsequent step-size lemma.
4. **Warm-start verification for general states.** To decouple verification from the assumption of an exact eigenstate warm start, we prove a one-step *propagation* inequality:

$$\sigma_\psi(\lambda^+) \leq \sigma_\psi(\lambda) + |\delta\lambda| \sigma_\psi(H_f - H_i),$$

based on a covariance bound (Cauchy–Schwarz). This yields a directly checkable sufficient condition for unique branch identification and (constant) fidelity at λ^+ from measurements at λ . This is done in Lemmas 12–13 and Corollary 2.

5. **Coupling verification to PL tracking.** Finally, we combine the verification certificate with the PL-based contraction guarantee from the optimization analysis: if the warm start is certified to lie on the round branch at λ^+ and the PL region drifts continuously, then (i) the same parameters remain inside the PL region at λ^+ and (ii) subsequent gradient steps contract toward $\theta^*(\lambda^+)$. This yields a *self-verified* adiabatic update rule. This combination is formalized in Theorem 4.

S5.2. Lemmas and corollaries

Variance as an eigen-branch identifier

Lemma 8 (Standard deviation identifies a unique ground state). *For any λ and any normalized state $|\psi\rangle$, there exists an index j such that*

$$|E_\psi(\lambda) - E_j(\lambda)| \leq \sigma_\psi(\lambda). \quad (\text{S5.215})$$

If $\sigma_\psi(\lambda) < \Delta_{\min}/2$, then this index j is unique.

Proof. Let $p_j = \langle \psi | \Pi_j(\lambda) | \psi \rangle$. Then

$$\sigma_\psi(\lambda)^2 = \sum_{j \geq 0} p_j (E_j(\lambda) - E_\psi(\lambda))^2.$$

If $|E_j - E_\psi| > \sigma_\psi$ for all j , then

$$\sigma_\psi^2 > \sum_j p_j \sigma_\psi^2 = \sigma_\psi^2,$$

is a contradiction. Hence, at least one index j satisfies the bound. If two distinct indices $j \neq k$ satisfy $|E_{j,k} - E_\psi| \leq \sigma_\psi$, then

$$|E_j - E_k| \leq |E_j - E_\psi| + |E_k - E_\psi| \leq 2\sigma_\psi$$

. If $\sigma_\psi < \Delta_{\min}/2$ then the two eigenbranches j, k satisfy:

$$|E_j - E_k| < \Delta_{\min}$$

contradicting Assumption 4 (assuming additionally that the gap also holds for j -th eigenstate, i.e. $j = j_*$). \square

Fidelity certification for the identified eigen-branch

Lemma 9 (Standard deviation-to-fidelity bound for the identified branch). *Fix λ and a normalized state $|\psi\rangle$. Assume $\sigma_\psi(\lambda) < \Delta_{\min}/2$ and let j_* be the unique index from Lemma 8, i.e.*

$$|E_\psi(\lambda) - E_{j_*}(\lambda)| \leq \sigma_\psi(\lambda).$$

Then

$$1 - \langle \psi | \Pi_{j_*}(\lambda) | \psi \rangle \leq \frac{\sigma_\psi(\lambda)^2}{(\Delta_{\min} - \sigma_\psi(\lambda))^2}. \quad (\text{S5.216})$$

Proof. Expand $|\psi\rangle$ in the eigenbasis of $H(\lambda)$: $|\psi\rangle = \sum_j \alpha_j |E_j(\lambda)\rangle$ with $p_j = |\alpha_j|^2 = \langle \psi | \Pi_j | \psi \rangle$. Then

$$\sigma_\psi(\lambda)^2 = \sum_j p_j (E_j(\lambda) - E_\psi(\lambda))^2.$$

Split the sum into the identified branch j_* and its complement:

$$\sigma_\psi(\lambda)^2 = p_{j_*} (E_{j_*} - E_\psi)^2 + \sum_{j \neq j_*} p_j (E_j - E_\psi)^2 \geq \sum_{j \neq j_*} p_j (E_j - E_\psi)^2,$$

where we used the fact that each term is positive. For any $j \neq j_*$,

$$|E_j - E_\psi| \geq |E_j - E_{j_*}| - |E_{j_*} - E_\psi| \geq \Delta_{\min} - \sqrt{V_\psi(\lambda)},$$

where we used Assumption 4 and the definition of j_* . Therefore,

$$\sigma_\psi(\lambda)^2 \geq \sum_{j \neq j_*} p_j (\Delta_{\min} - \sigma_\psi(\lambda))^2 = (1 - p_{j_*}) (\Delta_{\min} - \sigma_\psi(\lambda))^2.$$

Rearranging yields (S5.216). \square

Corollary 1 (Ground-state fidelity once the branch is known). *Under Assumption 4, suppose that the unique index j_* in Lemma 8 equals 0, i.e., we consider the ground state. If $\sigma_\psi(\lambda) \leq \Delta_{\min}/4$, then*

$$\langle \psi | \Pi_0(\lambda) | \psi \rangle \geq \frac{8}{9}.$$

Proof. Apply Lemma 9 with $j_* = 0$. If $\sigma_\psi \leq \Delta_{\min}/4$, then $\Delta_{\min} - \sigma_\psi \geq 3\Delta_{\min}/4$, giving the stated bound. \square

We stress that $\Delta_{\min}/4$ is an arbitrary value and any $\sigma < \Delta_{\min}/2$ would be feasible.

Exact warm-start variance for linear schedules

Lemma 10 (Exact warm-start standard deviation). *Let $|0(\lambda)\rangle$ denote the ground state of $H(\lambda)$. Then for any $\delta\lambda$,*

$$\sigma_{0(\lambda)}(H(\lambda + \delta\lambda))^2 = \delta\lambda^2 \sigma_{0(\lambda)}(H_f - H_i)^2. \quad (\text{S5.217})$$

Proof. Using $H(\lambda + \delta\lambda) = H(\lambda) + \delta\lambda(H_f - H_i)$ and $H(\lambda)|0(\lambda)\rangle = E_0(\lambda)|0(\lambda)\rangle$, all zeroth- and first-order contributions cancel in the variance expansion, leaving only the quadratic term. \square

Lemma 11 (Verification step-size bound). *If*

$$|\delta\lambda| < \frac{\Delta_{\min}}{2\sigma_{0(\lambda)}(H_f - H_i)},$$

then

$$\sigma_{0(\lambda)}(H(\lambda + \delta\lambda)) < \frac{\Delta_{\min}}{2}.$$

Consequently, the warm-start state $|0(\lambda)\rangle$ has overlap at least $8/9$ with the unique eigen-branch of $H(\lambda + \delta\lambda)$ identified by Lemma 8. If this branch is the ground branch, then the overlap with the actual ground state is at least $8/9$.

Proof. The standard deviation bound follows directly from Lemma 10. Since $\sqrt{V} < \Delta_{\min}/2$, Lemma 8 and Lemma 9 apply, yielding the stated fidelity bounds. \square

Standard deviation propagation for a general warm start

Lemma 12 (Covariance bound). *For any Hermitian operators A, B and any normalized state $|\psi\rangle$,*

$$|\text{Cov}_\psi(A, B)| = |\langle\psi|AB|\psi\rangle - \langle\psi|A|\psi\rangle\langle\psi|B|\psi\rangle| \leq \sigma_\psi(A)\sigma_\psi(B).$$

Proof. Let

$$\bar{A} = \langle\psi|A|\psi\rangle, \quad \bar{B} = \langle\psi|B|\psi\rangle,$$

and define the centered (Hermitian) operators

$$\tilde{A} = A - \bar{A}\mathbb{I}, \quad \tilde{B} = B - \bar{B}\mathbb{I}.$$

Then

$$\begin{aligned} \langle\psi|AB|\psi\rangle - \langle\psi|A|\psi\rangle\langle\psi|B|\psi\rangle &= \langle\psi|(A - \bar{A}\mathbb{I})(B - \bar{B}\mathbb{I})|\psi\rangle \\ &= \langle\psi|\tilde{A}\tilde{B}|\psi\rangle. \end{aligned} \quad (\text{S5.218})$$

Now set $|u\rangle = \tilde{A}|\psi\rangle$ and $|v\rangle = \tilde{B}|\psi\rangle$. By the Cauchy–Schwarz inequality,

$$|\langle\psi|\tilde{A}\tilde{B}|\psi\rangle| = |\langle u|v\rangle| \leq \|u\|\|v\|.$$

Moreover,

$$\|u\|^2 = \langle\psi|\tilde{A}^2|\psi\rangle = \langle\psi|(A - \bar{A}\mathbb{I})^2|\psi\rangle = \sigma_\psi(A)^2,$$

and similarly $\|v\|^2 = \sigma_\psi(B)^2$. Combining these identities with (S5.218) yields

$$|\langle\psi|AB|\psi\rangle - \langle\psi|A|\psi\rangle\langle\psi|B|\psi\rangle| \leq \sigma_\psi(A)\sigma_\psi(B),$$

which proves the claim. \square

Lemma 13 (One-step standard deviation propagation). *For any state $|\psi\rangle$ and any $\lambda, \delta\lambda$,*

$$\sigma_\psi(\lambda + \delta\lambda) \leq \sigma_\psi(\lambda) + |\delta\lambda|\sigma_\psi(H_f - H_i).$$

Proof. Write

$$H(\lambda + \delta\lambda) = H(\lambda) + \delta\lambda\mathcal{D}, \quad \mathcal{D} = H_f - H_i.$$

Denote expectation values with respect to $|\psi\rangle$ by $\langle \cdot \rangle = \langle \psi | (\cdot) | \psi \rangle$. Then

$$\sigma_\psi(\lambda + \delta\lambda)^2 = \langle (H + \delta\lambda\mathcal{D})^2 \rangle - \langle H + \delta\lambda\mathcal{D} \rangle^2.$$

Expanding and regrouping terms yields

$$\begin{aligned} \sigma_\psi(\lambda + \delta\lambda)^2 &= \underbrace{(\langle H^2 \rangle - \langle H \rangle^2)}_{= V_\psi(\lambda)} + 2\delta\lambda(\langle HD \rangle - \langle H \rangle \langle D \rangle) + \delta\lambda^2(\langle D^2 \rangle - \langle D \rangle^2) \\ &= \sigma_\psi(\lambda)^2 + 2\delta\lambda \text{Cov}_\psi(H, \mathcal{D}) + \delta\lambda^2 \sigma_\psi(\mathcal{D})^2. \end{aligned} \quad (\text{S5.219})$$

By Lemma 12,

$$|\text{Cov}_\psi(H, \mathcal{D})| \leq \sigma_\psi(H) \sigma_\psi(\mathcal{D}) = \sigma_\psi(\lambda) \sigma_\psi(\mathcal{D}).$$

Inserting this bound into (S5.219) gives

$$\sigma_\psi(\lambda + \delta\lambda)^2 \leq \sigma_\psi(\lambda)^2 + 2|\delta\lambda| \sigma_\psi(\lambda) \sigma_\psi(\mathcal{D}) + \delta\lambda^2 \sigma_\psi(\mathcal{D})^2 = (\sigma_\psi(\lambda) + |\delta\lambda| \sigma_\psi(\mathcal{D}))^2.$$

Taking square roots on both sides yields

$$\sigma_\psi(\lambda + \delta\lambda) \leq \sigma_\psi(\lambda) + |\delta\lambda| \sigma_\psi(H_f - H_i),$$

which proves the claim. \square

Corollary 2 (Verification condition). *If*

$$\sigma_\psi(\lambda) + |\delta\lambda| \sigma_\psi(H_f - H_i) < \frac{\Delta_{\min}}{2}.$$

In particular, there exists a unique eigen-branch j_\star at $\lambda + \delta\lambda$ such that

$$\langle \psi | \Pi_{j_\star}(\lambda + \delta\lambda) | \psi \rangle \geq 8/9.$$

If $j_\star = 0$, this certifies overlap $\geq 8/9$ with the actual ground state.

Verification combined with PL tracking

Theorem 4 (Certified evolution from PL entry and branch verification). *Fix λ and $\lambda^+ = \lambda + \delta\lambda$. Let $\boldsymbol{\theta}$ be parameters at λ with prepared state $|\psi\rangle = |\psi(\boldsymbol{\theta})\rangle$. Define*

$$\delta\lambda_A = \frac{\gamma^2 \Delta_{\min}^2}{24 \|H\|_{\text{op}} M^2 \|H_f - H_i\|_{\text{op}}}, \quad \delta\lambda_V = \frac{\Delta_{\min}/2 - \sigma_\psi(\lambda)}{\sigma_\psi(H_f - H_i)}.$$

Assume:

1. $j_\star = 0$;
2. $\sigma_\psi(\lambda) \leq \Delta_{\min}/2$;
3. $\boldsymbol{\theta}$ lies inside the PL region at λ ;
4. $|\delta\lambda| \leq \min\{\delta\lambda_A, \delta\lambda_V\}$.

Then:

1. $|\psi\rangle$ has overlap at least $8/9$ with a unique ground-state branch of $H(\lambda^+)$;
2. the same parameters $\boldsymbol{\theta}$ lie inside the PL region at λ^+ ;

3. gradient update steps at λ^+ contract toward $\boldsymbol{\theta}^*(\lambda^+)$;
4. if after optimization at λ^+ the algorithm enforces $\sigma_{\psi(\boldsymbol{\theta}_{\text{out}})}(\lambda^+) \leq \Delta_{\min}/2$, then the output state remains on the same eigen-branch with overlap at least $8/9$.

Proof. Because $|\delta\lambda| \leq \delta\lambda_V$, the propagated variance bound

$$\sigma_{\psi}(\lambda^+) \leq \sigma_{\psi}(\lambda) + |\delta\lambda| \sigma_{\psi}(H_f - H_i)$$

implies $\sigma_{\psi}(\lambda^+) < \Delta_{\min}/2$, so Corollary 2 yields (1).

Because $|\delta\lambda| \leq \delta\lambda_A$, the drift bound $\|\boldsymbol{\theta}^*(\lambda^+) - \boldsymbol{\theta}^*(\lambda)\| \leq D|\delta\lambda|$ and the triangle inequality imply that $\boldsymbol{\theta}$ remains within the PL radius at λ^+ , giving (2). Statement (3) is the standard PL–Euler contraction. Finally, (4) again follows from Corollary 2. \square

S6. EXTENSION TO ϵ -EXACT REPRESENTABILITY

In the previous analysis, we assumed exact representability of the instantaneous ground state along the adiabatic path. We now relax this assumption and show that the tracking and certification results extend naturally to the case of approximate representability.

ϵ -exact representability

We replace Assumption 2 by the following weaker condition.

Assumption 5 (ϵ -exact representability). *There exists a constant $\epsilon \geq 0$ such that for all $\lambda \in [0, 1]$ there exists parameters $\bar{\theta}(\lambda)$ satisfying*

$$E_{\lambda}(\bar{\theta}(\lambda)) \leq E_0(\lambda) + \epsilon, \quad (\text{S6.220})$$

where $E_0(\lambda)$ denotes the exact ground-state energy.

Define the variational optimum

$$\theta^{\text{opt}}(\lambda) \in \arg \min_{\theta} E_{\lambda}(\theta), \quad E_{\lambda}^{\text{opt}} = E_{\lambda}(\theta^{\text{opt}}(\lambda)). \quad (\text{S6.221})$$

By the variational principle,

$$0 \leq E_{\lambda}^{\text{opt}} - E_0(\lambda) \leq \epsilon. \quad (\text{S6.222})$$

Thus, in the absence of exact representability, optimization targets the best achievable variational approximation rather than the exact ground state.

Ground-state fidelity and representability bias

Approximate representability affects only statements that attempt to infer ground-state fidelity from optimization alone. Using the gap bound $\Delta_{\min}(\lambda) \geq \Delta_c > 0$ and the spectral decomposition of $H(\lambda)$, any normalized state $|\psi\rangle$ satisfies

$$1 - |\langle \psi_0(\lambda) | \psi \rangle|^2 \leq \frac{\langle H(\lambda) \rangle_{\psi} - E_0(\lambda)}{\Delta_c}. \quad (\text{S6.223})$$

Applying this bound to the variational optimum yields

$$|\langle \psi_0(\lambda) | \psi(\theta^{\text{opt}}(\lambda)) \rangle|^2 \geq 1 - \frac{\epsilon}{\Delta_c}. \quad (\text{S6.224})$$

This term represents an intrinsic expressibility bias that cannot be removed by optimization.

PL tracking under approximate representability

Under ϵ -exact representability, the variational minimizer $\theta^{\text{opt}}(\lambda)$ no longer corresponds to the exact ground state, but the local curvature remains strictly positive provided the representability bias is smaller than the spectral gap.

Evaluating the Hessian at $\theta^{\text{opt}}(\lambda)$ and using $E_{\lambda}^{\text{opt}} - E_0(\lambda) \leq \epsilon$ yields

$$\nabla^2 E_{\lambda}(\theta^{\text{opt}}(\lambda)) \succeq 2\gamma(\Delta_{\min} - \epsilon)I. \quad (\text{S6.225})$$

Hence, the effective PL constant becomes

$$\mu_{\text{eff}} = \gamma(\Delta_{\min} - \epsilon), \quad (\text{S6.226})$$

and the PL radius is reduced to

$$r_{\text{PL}}^{(\epsilon)} = \frac{\gamma(\Delta_{\min} - \epsilon)}{L_H}. \quad (\text{S6.227})$$

The reduced PL radius also reduces the admissible $\delta\lambda$

$$|\delta\lambda| \leq \delta\lambda_{\text{A}}^{(\epsilon)} = \frac{\gamma^2(\Delta_{\min} - \epsilon)^2}{L_H \sqrt{M} \|\partial_{\lambda} H\|_{\text{op}}}. \quad (\text{S6.228})$$

Under the condition

$$\epsilon < \Delta_{\min}, \quad (\text{S6.229})$$

the PL region remains nondegenerate. All PL tracking lemmas and theorems of the supplement then hold as stated with two changes: $\theta^*(\lambda)$ replaced by $\theta^{\text{opt}}(\lambda)$, and the substitution

$$\Delta_{\min} \longrightarrow \Delta_{\min} - \epsilon. \quad (\text{S6.230})$$

Thus, approximate representability reduces the effective curvature, shrinks the PL region, and tightens the admissible adiabatic step size through the replacement of Δ_{\min} by $\Delta_{\min} - \epsilon$.

Verification guarantees remain unchanged

The variance-based certification results of Corollary 2 are purely spectral and do not rely on exact representability. Therefore, if the standard-deviation condition $\sigma_{\psi}(H(\lambda)) < \Delta_c/2$ holds, the prepared state obeys

$$|\langle \psi_0(\lambda) | \psi(\theta) \rangle|^2 \geq \frac{8}{9}, \quad (\text{S6.231})$$

independently of ϵ . In particular, approximate representability modifies only the tracking interpretation (optimization toward θ^{opt}) but does not degrade the certified fidelity bound obtained from runtime verification.

Admissible range of the representability error

The representability error ϵ determines whether the variance-based certification condition can be satisfied. Certification requires

$$\sigma_{\psi}(H(\lambda)) < \frac{\Delta_c}{2}, \quad (\text{S6.232})$$

equivalently,

$$\text{Var}_{\psi}(H(\lambda)) < \frac{\Delta_c^2}{4}. \quad (\text{S6.233})$$

Suppose the variational ansatz has representability bias $E_\lambda^{\text{opt}} - E_0(\lambda) \leq \epsilon$. This bias induces a nonzero minimum achievable variance. Using the spectral decomposition

$$H(\lambda) = \sum_{j \geq 0} E_j(\lambda) \Pi_j(\lambda), \quad p_j = \langle \psi | \Pi_j(\lambda) | \psi \rangle,$$

define shifted excitation energies

$$\delta_j := E_j(\lambda) - E_0(\lambda).$$

Since variance is invariant under constant shifts,

$$\text{Var}_\psi(H(\lambda)) = \sum_{j \geq 0} p_j \delta_j^2 - \left(\sum_{j \geq 0} p_j \delta_j \right)^2.$$

The gap condition implies $\delta_0 = 0$ and $\delta_j \geq \Delta_c$ for all $j \geq 1$. Because $\delta_j \in \{0\} \cup [\Delta_c, \infty)$, we have $\delta_j^2 \geq \Delta_c \delta_j$ for all j . Hence,

$$\sum_{j \geq 0} p_j \delta_j^2 \geq \Delta_c \sum_{j \geq 0} p_j \delta_j = \Delta_c (\langle H(\lambda) \rangle_\psi - E_0(\lambda)). \quad (\text{S6.234})$$

Dropping the second (negative) square term yields

$$\text{Var}_\psi(H(\lambda)) \geq \Delta_c (\langle H(\lambda) \rangle_\psi - E_0(\lambda)). \quad (\text{S6.235})$$

Applying this bound to the variational optimum gives

$$\text{Var}_{\text{opt}}(H(\lambda)) \geq \Delta_c (E_\lambda^{\text{opt}} - E_0(\lambda)) \geq \Delta_c \epsilon. \quad (\text{S6.236})$$

Therefore,

$$\sigma_{\text{opt}}(H(\lambda)) \geq \sqrt{\Delta_c \epsilon}. \quad (\text{S6.237})$$

Certification requires $\sigma_\psi(H(\lambda)) < \Delta_c/2$. Thus, certification can be satisfied whenever

$$\sqrt{\Delta_c \epsilon} \leq \frac{\Delta_c}{2}, \quad (\text{S6.238})$$

i.e.

$$\epsilon \leq \frac{\Delta_c}{4}, \quad (\text{S6.239})$$

which is the upper bound on the ϵ -representability error discussed in the main text, since the tracking restriction is less strict.

S7. MEASUREMENT COST AND STABILITY UNDER SHOT NOISE

In realistic implementations, gradients of the variational energy are not evaluated precisely but are estimated from a finite number of projective measurements on quantum hardware. In this section, we quantify how the required measurement (shot) budget must scale with problem parameters in order to guarantee, with high probability, that (i) all optimization iterates remain inside the local Polyak–Łojasiewicz (PL) region used in the adiabatic tracking analysis, and (ii) the iterates converge toward the *correct* instantaneous variational minimizer along the adiabatic path.

Throughout this section, M denotes the number of variational parameters and \mathcal{K} denotes the number of Pauli measurement terms (or commuting measurement groups) in the Hamiltonian decomposition. We use the explicit PL radius established in previous sections,

$$r_{\text{PL}} = \frac{\gamma \Delta_{\min}}{L_H}, \quad L_H = 24 \|H\|_{\text{op}} M^{3/2}. \quad (\text{S7.240})$$

S7.1. Stochastic gradient model induced by finite shot count

Fix an adiabatic parameter λ and consider the variational energy

$$E_\lambda(\boldsymbol{\theta}) = \langle \psi(\boldsymbol{\theta}) | H(\lambda) | \psi(\boldsymbol{\theta}) \rangle, \quad H(\lambda) = \sum_{\ell=1}^K h_\ell(\lambda) P_\ell,$$

where P_ℓ are Pauli operators defined in the setup Section S1. Using the parameter-shift rule, gradient descent updates take the stochastic form

$$\boldsymbol{\theta}^{(k+1)} = \boldsymbol{\theta}^{(k)} - \eta (\nabla E_\lambda(\boldsymbol{\theta}^{(k)}) + \xi_k), \quad (\text{S7.241})$$

where ξ_k denotes the gradient estimation error induced by finite measurement shots. We assume

$$\mathbb{E}[\xi_k | \boldsymbol{\theta}^{(k)}] = 0, \quad \mathbb{E}\left[\|\xi_k\|_2^2 | \boldsymbol{\theta}^{(k)}\right] \leq \sigma^2(S), \quad (\text{S7.242})$$

where S is the number of shots per Hamiltonian term. For Pauli measurements with independent shot noise, we can derive an explicit bound on the variance of a single energy estimate. Fix λ and $\boldsymbol{\theta}$ and write

$$E_\lambda(\boldsymbol{\theta}) = \sum_{\ell=1}^K h_\ell(\lambda) \langle P_\ell \rangle_{\boldsymbol{\theta}, \lambda},$$

where $\langle P_\ell \rangle_{\boldsymbol{\theta}, \lambda} = \langle \psi(\boldsymbol{\theta}) | P_\ell | \psi(\boldsymbol{\theta}) \rangle \in [-1, 1]$. Assume we estimate each Pauli expectation value $\langle P_\ell \rangle_{\boldsymbol{\theta}, \lambda}$ by performing S shots of the measurement of P_ℓ , yielding outcomes $X_{\ell,1}, \dots, X_{\ell,S} \in \{+1, -1\}$ with

$$\mathbb{E}[X_{\ell,s}] = \langle P_\ell \rangle_{\boldsymbol{\theta}, \lambda}, \quad \text{Var}(X_{\ell,s}) = 1 - \langle P_\ell \rangle_{\boldsymbol{\theta}, \lambda}^2 \leq 1.$$

Define the sample mean estimator

$$\widehat{\langle P_\ell \rangle} = \frac{1}{S} \sum_{s=1}^S X_{\ell,s}, \quad \widehat{E_\lambda(\boldsymbol{\theta})} = \sum_{\ell=1}^K h_\ell(\lambda) \widehat{\langle P_\ell \rangle}.$$

Then $\widehat{E_\lambda(\boldsymbol{\theta})}$ is unbiased:

$$\mathbb{E}\left[\widehat{E_\lambda(\boldsymbol{\theta})}\right] = \sum_{\ell=1}^K h_\ell(\lambda) \mathbb{E}\left[\widehat{\langle P_\ell \rangle}\right] = \sum_{\ell=1}^K h_\ell(\lambda) \langle P_\ell \rangle_{\boldsymbol{\theta}, \lambda} = E_\lambda(\boldsymbol{\theta}).$$

To bound the variance, first note that, by independence of shots for a fixed ℓ ,

$$\text{Var}\left(\widehat{\langle P_\ell \rangle}\right) = \text{Var}\left(\frac{1}{S} \sum_{s=1}^S X_{\ell,s}\right) = \frac{1}{S^2} \sum_{s=1}^S \text{Var}(X_{\ell,s}) = \frac{1}{S} \text{Var}(X_{\ell,1}) = \frac{1 - \langle P_\ell \rangle_{\boldsymbol{\theta}, \lambda}^2}{S} \leq \frac{1}{S}.$$

Next, assume that the estimators $\widehat{\langle P_\ell \rangle}$ are obtained from independent measurement data across different ℓ (e.g. by allocating disjoint shot batches per term or per commuting group). Then the random variables $\widehat{\langle P_\ell \rangle}$ are independent, and therefore

$$\text{Var}\left[\widehat{E_\lambda(\boldsymbol{\theta})}\right] = \text{Var}\left[\sum_{\ell=1}^K h_\ell(\lambda) \widehat{\langle P_\ell \rangle}\right] = \sum_{\ell=1}^K h_\ell(\lambda)^2 \text{Var}\left(\widehat{\langle P_\ell \rangle}\right) \quad (\text{S7.243})$$

$$\leq \sum_{\ell=1}^K h_\ell(\lambda)^2 \cdot \frac{1}{S} = \frac{1}{S} \sum_{\ell=1}^K h_\ell(\lambda)^2 = \frac{\|h(\lambda)\|_2^2}{S}, \quad (\text{S7.244})$$

where we defined

$$\|h(\lambda)\|_2^2 = \sum_{\ell=1}^K h_\ell(\lambda)^2.$$

If measurements are grouped into commuting sets, the same derivation holds with ℓ indexing the groups and $h_\ell(\lambda) P_\ell$ replaced by the corresponding grouped observable.

A full parameter-shift gradient requires $2M$ energy evaluations. Summing the variances of the gradient components yields

$$\sigma^2(S) \leq \frac{2M \sup_{\lambda \in [0,1]} \|h(\lambda)\|_2^2}{S}. \quad (\text{S7.245})$$

S7.2. High-probability invariance of the PL region (never leave PL region)

Fix λ and write $\boldsymbol{\theta}^* = \boldsymbol{\theta}_\lambda^*$. Throughout this section, we work inside the PL region (see Lemma 5)

$$\mathcal{D}_\lambda = \{\boldsymbol{\theta} : \|\boldsymbol{\theta} - \boldsymbol{\theta}^*\|_2 \leq r_{\text{PL}}\}, \quad r_{\text{PL}} = \frac{\gamma \Delta_{\min}}{L_H}, \quad \mu = \gamma \Delta_{\min},$$

Consider the stochastic update

$$\boldsymbol{\theta}^{(k+1)} = \boldsymbol{\theta}^{(k)} - \eta (\nabla E_\lambda(\boldsymbol{\theta}^{(k)}) + \xi_k), \quad \eta \leq \frac{1}{L}, \quad (\text{S7.246})$$

where L is the smoothness constant defined in Lemma 2.

By the triangle inequality applied to (S7.246),

$$\begin{aligned} \|\boldsymbol{\theta}^{(k+1)} - \boldsymbol{\theta}^*\|_2 &= \|\boldsymbol{\theta}^{(k)} - \boldsymbol{\theta}^* - \eta \nabla E_\lambda(\boldsymbol{\theta}^{(k)}) - \eta \xi_k\|_2 \\ &\leq \underbrace{\|\boldsymbol{\theta}^{(k)} - \boldsymbol{\theta}^* - \eta \nabla E_\lambda(\boldsymbol{\theta}^{(k)})\|_2}_{\text{noiseless GD step}} + \eta \|\xi_k\|_2. \end{aligned} \quad (\text{S7.247})$$

Inside \mathcal{D}_λ , PL+smoothness implies that gradient descent with $\eta \leq 1/L$ is contractive in distance to $\boldsymbol{\theta}^*$ (see Lemma 7):

$$\|\boldsymbol{\theta}^{(k)} - \boldsymbol{\theta}^* - \eta \nabla E_\lambda(\boldsymbol{\theta}^{(k)})\|_2 \leq \sqrt{1 - \eta \mu} \|\boldsymbol{\theta}^{(k)} - \boldsymbol{\theta}^*\|_2. \quad (\text{S7.248})$$

Combining (S7.247)–(S7.248) and using $\|\boldsymbol{\theta}^{(k)} - \boldsymbol{\theta}^*\|_2 \leq r_{\text{PL}}$ gives

$$\|\boldsymbol{\theta}^{(k+1)} - \boldsymbol{\theta}^*\|_2 \leq \sqrt{1 - \eta \mu} r_{\text{PL}} + \eta \|\xi_k\|_2.$$

Thus $\|\boldsymbol{\theta}^{(k+1)} - \boldsymbol{\theta}^*\|_2 \leq r_{\text{PL}}$ is guaranteed whenever $\sqrt{1 - \eta \mu} r_{\text{PL}} + \eta \|\xi_k\|_2 < r_{\text{PL}}$. For small $\eta \mu$ we find

$$\|\xi_k\|_2 < \frac{1}{2} \mu r_{\text{PL}}. \quad (\text{S7.249})$$

This condition is *tight*; if $\|\xi_k\|_2 > \frac{1}{2} \mu r_{\text{PL}}$, then for a point on the boundary $\|\boldsymbol{\theta}^{(k)} - \boldsymbol{\theta}^*\|_2 = r_{\text{PL}}$ the upper bound Eq. S7.247 exceeds r_{PL} , so one-step invariance cannot be ensured uniformly over all boundary points.

High-probability enforcement via Gaussian norm concentration.

Assume that, conditionally on $\boldsymbol{\theta}^{(k)}$, the gradient noise is Gaussian with mean zero and isotropic covariance chosen so that it matches the variance proxy in (S7.242):

$$\xi_k \mid \boldsymbol{\theta}^{(k)} \sim \mathcal{N}\left(0, \frac{\sigma^2(S)}{M} I_M\right), \quad \text{so that} \quad \mathbb{E}\left[\|\xi_k\|_2^2 \mid \boldsymbol{\theta}^{(k)}\right] = \sigma^2(S). \quad (\text{S7.250})$$

Equivalently, we may write $\xi_k = \frac{\sigma(S)}{\sqrt{M}} g_k$ with $g_k \sim \mathcal{N}(0, I_M)$. Since the map $g \mapsto \|g\|_2$ is 1-Lipschitz and g_k is standard Gaussian, we have for all $x \geq 0$

$$\mathbb{P}\left(\|g_k\|_2 \geq \mathbb{E}\|g_k\|_2 + \sqrt{2x}\right) \leq e^{-x}. \quad (\text{S7.251})$$

Moreover, $\mathbb{E}\|g_k\|_2 \leq \sqrt{M}$. Therefore, for all $x \geq 0$,

$$\mathbb{P}\left(\|g_k\|_2 \geq \sqrt{M} + \sqrt{2x}\right) \leq e^{-x}. \quad (\text{S7.252})$$

Rescaling back to $\xi_k = \frac{\sigma(S)}{\sqrt{M}} g_k$ yields

$$\mathbb{P}\left(\|\xi_k\|_2 \geq \sigma(S) \left(1 + \sqrt{\frac{2x}{M}}\right) \mid \boldsymbol{\theta}^{(k)}\right) \leq e^{-x}. \quad (\text{S7.253})$$

Set $x = \log(K/\delta)$. Then (S7.253) gives

$$\mathbb{P}\left(\|\xi_k\|_2 \geq \sigma(S)\left(1 + \sqrt{\frac{2\log(K/\delta)}{M}}\right) \mid \boldsymbol{\theta}^{(k)}\right) \leq \frac{\delta}{K}.$$

Applying a union bound over $k = 0, \dots, K-1$, we obtain that with probability at least $1 - \delta$,

$$\|\xi_k\|_2 \leq \sigma(S)\left(1 + \sqrt{\frac{2\log(K/\delta)}{M}}\right) \quad \text{for all } k = 0, \dots, K-1. \quad (\text{S7.254})$$

Combining (S7.254) with the deterministic invariance condition $\|\xi_k\|_2 < \frac{1}{2}\mu r_{\text{PL}}$ from Eq. S7.249, it suffices that

$$\sigma(S)\left(1 + \sqrt{\frac{2\log(K/\delta)}{M}}\right) \leq \frac{1}{2}\mu r_{\text{PL}}. \quad (\text{S7.255})$$

Equivalently,

$$\sigma(S) \leq \frac{1}{2} \frac{\mu r_{\text{PL}}}{1 + \sqrt{\frac{2\log(K/\delta)}{M}}}. \quad (\text{S7.256})$$

Using the parameter-shift variance proxy $\sigma^2(S) \leq \frac{2M \sup_{\lambda} \|h(\lambda)\|_2^2}{S}$, a sufficient shot budget is therefore

$$S \geq \frac{8M \sup_{\lambda} \|h(\lambda)\|_2^2}{\mu^2 r_{\text{PL}}^2} \left(1 + \sqrt{\frac{2\log(K/\delta)}{M}}\right)^2. \quad (\text{S7.257})$$

Substituting $\mu = \gamma\Delta_{\min}$ and $r_{\text{PL}} = \gamma\Delta_{\min}/L_H$ yields the gap scaling

$$\boxed{S \geq \frac{8M \sup_{\lambda} \|h(\lambda)\|_2^2 L_H^2}{\gamma^4 \Delta_{\min}^4} \left(1 + \sqrt{\frac{2\log(K/\delta)}{M}}\right)^2}. \quad (\text{S7.258})$$

In particular, the leading dependence on the spectral gap is $S \propto \Delta_{\min}^{-4}$.

S7.3. Total measurement cost

Each parameter-shift gradient evaluation requires $2M$ energy measurements. Each energy measurement consists of \mathcal{K} Pauli terms estimated with S shots. Therefore, the measurement cost per gradient step is

$$\mathcal{C}_{\text{iter}} = 2M\mathcal{K}S.$$

Over K gradient updates, the total measurement cost (for fixed λ) is

$$\mathcal{C}_{\text{total}} = 2KMS, \quad (\text{S7.259})$$

with S chosen according to (S7.258).

Summary

When the PL radius is fixed to its explicit value $r_{\text{PL}} = \gamma\Delta_{\min}/L_H$, finite-shot noise does not invalidate adiabatic PL-based tracking, provided the shot budget scales polynomially in M , K , and the inverse gap. With parameter-shift gradients, both high-probability invariance of the PL region and convergence to the correct instantaneous minimizer are guaranteed under an explicit and controlled measurement budget.

- [2] P. Hauke, H. G. Katzgraber, W. Lechner, H. Nishimori, and W. D. Oliver, Perspectives of quantum annealing: methods and implementations, *Rep. Prog. Phys.* **83**, 054401 (2020).
- [3] B. Žunkovič, P. Torta, G. Pecci, G. Lami, and M. Collura, Variational Ground-State Quantum Adiabatic Theorem, *Phys. Rev. Lett.* **134**, 130601 (2025).
- [4] E. Hairer and G. Wanner, *Solving Ordinary Differential Equations II*, Springer Series in Computational Mathematics, Vol. 14 (Springer, Berlin, Heidelberg, 1996).
- [5] H. Karimi, J. Nutini, and M. Schmidt, Linear Convergence of Gradient and Proximal-Gradient Methods Under the Polyak-Łojasiewicz Condition (2020), [arXiv:1608.04636 \[cs.LG\]](https://arxiv.org/abs/1608.04636).
- [6] A. M. Mathai and S. B. Provost, *Quadratic Forms in Random Variables: Theory and Applications*, Statistics: Textbooks and Monographs, Vol. 126 (Marcel Dekker, 1992).